

## Special Section:

Continuous Nutrient Sensing in Research and Management: Applications and Lessons Learned Across Aquatic Environments and Watersheds

## Key Points:

- Use of paired, in situ, high frequency nitrate sensors provided novel insights into nutrient sources and transformation rates
- Nitrification of wastewater-derived ammonium accounted for a large portion of the nitrate inventory in the Sacramento River
- Continuous measurements also revealed that a substantial benthic source of nitrate exists downstream of the wastewater treatment plant

## Supporting Information:

- Supporting Information S1

## Correspondence to:

T. E. C. Kraus,  
tkraus@usgs.gov

## Citation:

Kraus, T. E. C., O'Donnell, K., Downing, B. D., Bureau, J. R., & Bergamaschi, B. A. (2017). Using paired in situ high frequency nitrate measurements to better understand controls on nitrate concentrations and estimate nitrification rates in a wastewater-impacted river. *Water Resources Research*, 53, 8423–8442. <https://doi.org/10.1002/2017WR020670>

Received 28 FEB 2017

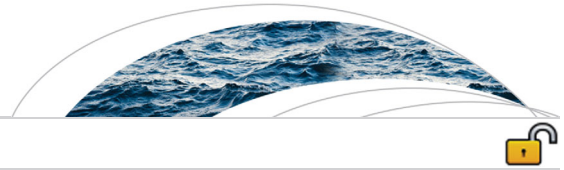
Accepted 6 SEP 2017

Accepted article online 13 SEP 2017

Published online 20 OCT 2017

© 2017. The Authors.

This is an open access article under the terms of the Creative Commons Attribution-NonCommercial-NoDerivs License, which permits use and distribution in any medium, provided the original work is properly cited, the use is non-commercial and no modifications or adaptations are made.



## Using Paired In Situ High Frequency Nitrate Measurements to Better Understand Controls on Nitrate Concentrations and Estimate Nitrification Rates in a Wastewater-Impacted River

T. E. C. Kraus<sup>1</sup> , K. O'Donnell<sup>1</sup> , B. D. Downing<sup>1</sup> , J. R. Bureau<sup>1</sup> , and B. A. Bergamaschi<sup>1</sup> 

<sup>1</sup>U.S. Geological Survey, California Water Science Center, Sacramento, CA, USA

**Abstract** We used paired continuous nitrate ( $\text{NO}_3^-$ ) measurements along a tidally affected river receiving wastewater discharge rich in ammonium ( $\text{NH}_4^+$ ) to quantify rates of change in  $\text{NO}_3^-$  concentration ( $R_{\Delta\text{NO}_3}$ ) and estimate nitrification rates.  $\text{NO}_3^-$  sensors were deployed 30 km apart in the Sacramento River, California (USA), with the upstream station located immediately above the regional wastewater treatment plant (WWTP). We used a travel time model to track water transit between the stations and estimated  $R_{\Delta\text{NO}_3}$  every 15 min (October 2013 to September 2014). Changes in  $\text{NO}_3^-$  concentration were strongly related to water temperature. In the presence of wastewater,  $R_{\Delta\text{NO}_3}$  was generally positive, ranging from about  $7 \mu\text{M d}^{-1}$  in the summer to near zero in the winter. Numerous periods when the WWTP halted discharge allowed the  $R_{\Delta\text{NO}_3}$  to be estimated under no-effluent conditions and revealed that in the absence of effluent, net gains in  $\text{NO}_3^-$  were substantially lower but still positive in the summer and negative (net sink) in the winter. Nitrification rates of effluent-derived  $\text{NH}_4^+$  ( $R_{\text{Nitrific}_E}$ ) were estimated from the difference between  $R_{\Delta\text{NO}_3}$  measured in the presence versus absence of effluent and ranged from  $1.5$  to  $3.4 \mu\text{M d}^{-1}$ , which is within literature values but tenfold greater than recently reported for this region.  $R_{\text{Nitrific}_E}$  was generally lower in winter ( $\sim 2 \mu\text{M d}^{-1}$ ) than summer ( $\sim 3 \mu\text{M d}^{-1}$ ). This in situ, high frequency approach provides advantages over traditional discrete sampling, incubation, and tracer methods and allows measurements to be made over broad areas for extended periods of time. Incorporating this approach into environmental monitoring programs can facilitate our ability to protect and manage aquatic systems.

**Plain Language Summary** The advent of in situ, high frequency nutrient sensors provides new opportunities to identify nutrient sources and quantify rates of transfer between different nutrient pools, improving our ability to assess how anthropogenic nutrient inputs affect aquatic ecosystems. We demonstrate how deployment of paired nitrate sensors along a tidally affected river which receives treated wastewater effluent rich in ammonium allowed us to quantify changes in nitrate concentration and, by identifying periods when effluent inputs were halted, estimate nitrification rates. Accurately quantifying nitrification rates enables us to approximate how much time it takes to deplete the ammonium pool and thus assess the fate and effects of effluent-derived nitrogen. In the Sacramento River, ammonium inputs from a wastewater treatment plant were rapidly nitrified and accounted for a large portion of the nitrate inventory entering the downstream estuary. Continuous measurements also revealed that a substantial benthic source of nitrate exists in the river reach below the treatment plant. This in situ approach avoids artifacts and logistical constraints associated with traditional approaches such as bottle incubations and tracer studies, providing environmentally relevant rates at high temporal and spatial resolution. Incorporating this approach into environmental monitoring programs will facilitate our ability to protect and manage aquatic systems.

### 1. Introduction

Nutrients—their concentration, form, and ratios—are key drivers of aquatic primary production, but at high concentrations nutrients can negatively impact water quality and ecosystem health (Paerl et al., 2016; Statham, 2012). While identifying nutrient sources and quantifying their fluxes will help us understand and manage freshwater and coastal systems, there is also a need to characterize dominant processes affecting nutrient pools as water is transported through the system. In particular, accurately quantifying rates will

allow us to ascertain how rapidly nutrient inputs from anthropogenic sources will be transformed and attenuated during transport, thus modulating effects on downstream ecosystems—a process often referred to as “nutrient spiraling” (e.g., Ensign & Doyle, 2006; Hensley et al., 2014; Pennino et al., 2016; Wollheim et al., 2008).

In many larger rivers and estuaries, excessive inputs of nitrogen from wastewater treatment plants (WWTPs) are linked to eutrophication, hypoxia, harmful algal blooms, and deleterious alterations to the food web (Aissa-Grouz et al., 2016; Paerl et al., 2014). The amount and form of nitrogen that WWTPs discharge depends on the treatment method employed. In the absence of a nitrification step, treated wastewater effluent is typically high in ammonium ( $\text{NH}_4^+$ ) and contains little to no nitrate ( $\text{NO}_3^-$ ) (Carey & Migliaccio, 2009). Plant nitrification can be expensive because conversion of  $\text{NH}_4^+$  to  $\text{NO}_3^-$  requires aerobic conditions, an active microbial nitrifying community, and sufficient time. When nitrification is not employed and concentrations of  $\text{NH}_4^+$  in treated effluent are elevated, the fate of  $\text{NH}_4^+$  in the receiving waters and the impact it has on downstream  $\text{NO}_3^-$  concentrations largely depends on the rate at which  $\text{NH}_4^+$  is nitrified in aerobic surface waters.

Accurate quantification of nitrification rates is important for four primary reasons. First, nitrification consumes oxygen and can be a major contributor to low dissolved oxygen conditions which is of great concern in many riverine, estuarine, and coastal habitats (Aissa-Grouz et al., 2016; Garnier et al., 2007). Second, conversion from  $\text{NH}_4^+$  to  $\text{NO}_3^-$  places nitrogen in a form that can be denitrified and thus subsequently removed from aquatic ecosystems, thereby ameliorating potential impacts from eutrophication (Damashek et al., 2016; Ensign & Doyle, 2006; Mulholland et al., 2009). Third, the concentration and form of inorganic nitrogen ( $\text{NO}_3^-$  versus  $\text{NH}_4^+$ ) may affect rates of primary production, phytoplankton abundance, and phytoplankton community composition, altering pelagic food webs (Glibert et al., 2016, and references therein). Further, high concentrations of ammonium may promote harmful algal blooms (Lehman et al., 2015; Paerl & Scott, 2010) and the spread of invasive aquatic vegetation (Luoma et al., 2015). Fourth, at high  $\text{NH}_4^+$  concentrations, unionized ammonia ( $\text{NH}_3$ ) and nitrite ( $\text{NO}_2^-$ ; an intermediate product of nitrification) can be toxic to fish and other aquatic organisms (Constable et al., 2003; Raimonet et al., 2015; Randall & Tsui, 2002).

Nitrification is a two-step process that first requires oxidation of  $\text{NH}_4^+$  to  $\text{NO}_2^-$  and then to  $\text{NO}_3^-$ . Both of these biologically mediated steps can be affected by a number of environmental conditions such as temperature, turbidity, salinity, pH, and oxygen availability, along with the quantity and composition of the nitrifying bacteria, availability of  $\text{NH}_4^+$  and organic carbon, and even light and  $\text{NO}_3^-$  concentrations (Bernhardt & Likens, 2002; Damashek et al., 2016; Shammas, 1986; Strauss et al., 2002, 2004). For this reason, it is useful to have nitrification-rate estimates over a wide variety of environmental conditions.

Quantifying rates of individual processes affecting nutrient pools within aquatic systems is particularly difficult because there are usually multiple processes occurring simultaneously. For example, a change in the  $\text{NO}_3^-$  pool over time (mass balance approach) is the net result of new inputs from nitrification, benthic release, and other sources (e.g., groundwater, tributary, or drainage water inflows) minus losses due to denitrification, dissimilatory  $\text{NO}_3^-$  reduction (DNR), and uptake by phytoplankton, microbes, vegetation, and other organisms living in the water column and the benthos (Figure 1). Traditional methods to specifically measure nitrification rates in the water column typically involve bottle incubations using isotopic tracers and/or inhibitors, which necessarily rely on a relatively limited number of samples and operationally defined conditions that may not always be representative of the natural environment (Andersson et al., 2006; Damashek et al., 2016). Bottle incubations also may not adequately capture the effects of particle bound nitrification when total suspended sediment concentrations change over short time periods, as is commonly found in tidal systems (Hsiao et al., 2014; Xia et al., 2009). Moreover, laboratory bottle incubations typically do not account for interactions with the benthos, which can vary over both time and space (Hensley et al., 2015; Strauss et al., 2004; Xia et al., 2008). Nitrification rates associated with sediments are typically determined in separate studies by collecting sediment cores and measuring changes in nutrient concentrations in the overlying water under laboratory controlled conditions (e.g., Ensign & Doyle, 2006). Extrapolating these rates to effects on water column nutrient concentrations requires assumptions about surface to water ratios (depth), water residence time, and boundary layer interactions.

Mass balance approaches employed in natural systems rely on parcel tracking or estimations of travel time between sampling points to calculate both absolute changes ( $\mu\text{M}$ ) and rates of change ( $\mu\text{M d}^{-1}$ ) in

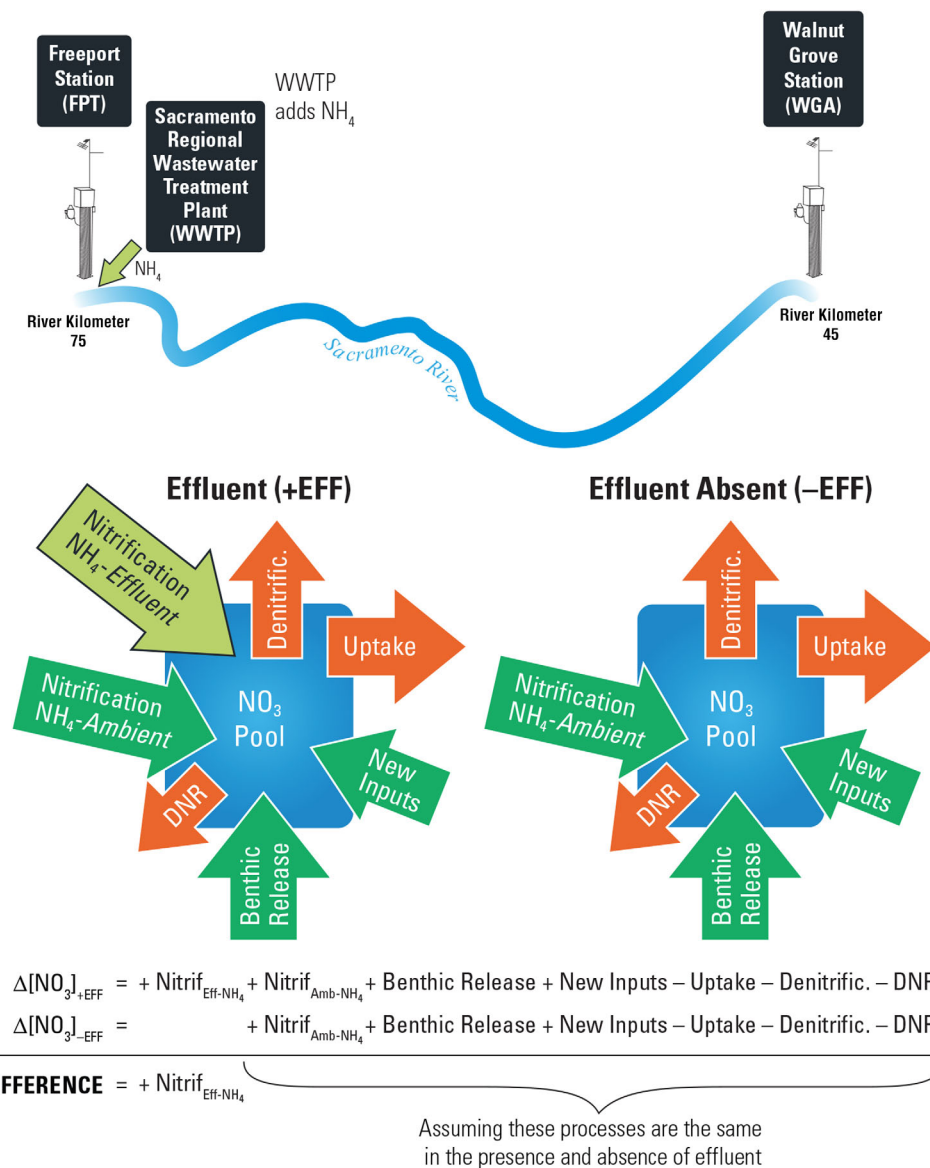


**Figure 1.** Conceptual diagram showing processes affecting the nitrate ( $\text{NO}_3^-$ ) pool as water transits down the Sacramento River between the Freeport (FPT) and Walnut Grove (WGA) high frequency monitoring stations in the absence of effluent ( $-\text{EFF}$ ) and presence of effluent ( $+\text{EFF}$ ). Assuming processes are the same under  $-\text{EFF}$  and  $+\text{EFF}$  conditions, and that effluent is the predominant source of  $\text{NH}_4^+$ , differences between changes in the  $\text{NO}_3^-$  pool can be attributed to nitrification of effluent-derived  $\text{NH}_4^+$ . Abbreviations:  $\text{NH}_4^+$ , ammonium; Nitrif., nitrification; Denitrific., denitrification; DNR, dissimilatory nitrate reduction.

constituent concentrations, which are particularly challenging in hydrologically complex systems such as tidally affected rivers and estuaries (Hensley et al., 2015; Kraus et al., 2017b). Tracer studies are informative, but due to logistical constraints their application is typically limited to smaller streams (Ensign & Doyle, 2006; Peterson et al., 2001; Tank et al., 2008). All of these approaches to characterizing nutrient transformation rates in aquatic systems rely on discrete sample collection, which limits the temporal and spatial resolution of these studies (Hensley et al., 2014; Rode et al., 2016b).

The advent of high frequency nutrient sensors that collect high temporal resolution data in situ is providing new opportunities to gain insight into the processes affecting nutrients (see reviews by Blaen et al., 2016; Kirchner et al., 2004; Kraus et al., 2017a; Pellerin et al., 2016; Rode et al., 2016a). For example, the use of in situ  $\text{NO}_3^-$  sensors has proven useful in other systems for characterizing short-term changes in  $\text{NO}_3^-$

concentration, more accurately calculating  $\text{NO}_3^-$  fluxes and loads, and for quantifying ecosystem  $\text{NO}_3^-$  uptake (e.g., Alexander et al., 2009; Crawford et al., 2015; Downing et al., 2016; Gilbert et al., 2013; Heffernan & Cohen, 2010; Hensley et al., 2014; Pellerin et al., 2009, 2014). Recent papers by Hensley et al. (2015) and Kunz et al. (2017) used paired sensors to look at  $\text{NO}_3^-$  removal during transport between two stations. In almost all cases, high frequency data reveal much higher variability in nutrient concentrations than was apparent from less-frequent discrete sample collection (e.g., Bende-Michl et al., 2013; Blaen et al., 2016; Pellerin et al., 2009, 2014; Rusjan & Mikos, 2010; Wild-Allen & Rayner, 2014). Colocating nutrient measurements with other high frequency data (e.g., discharge, velocity, temperature, specific conductance, dissolved oxygen, turbidity, pH, and chlorophyll) allows us to investigate environmental controls on these processes because they provide the means to make quantitative calculations related to, for example, changes in water quality, travel times, and fine-scale concentration changes (Heffernan & Cohen, 2010).

Here we present a new approach for calculating rates of change in  $\text{NO}_3^-$  concentration and for estimating nitrification rates using continuous, paired, in situ, high frequency  $\text{NO}_3^-$  sensors in a wastewater-impacted river by taking advantage of periods when the river was free of effluent inputs. The study was located in a tidal reach of the Sacramento River (CA, USA) using sensors deployed approximately 30 km apart. Immediately downstream of the upstream sensor station, the river receives effluent high in  $\text{NH}_4^+$  from the Sacramento Regional WWTP. Using colocated velocity and other water quality measurements, we determined the travel time between the two stations and quantified changes in  $\text{NO}_3^-$  concentration between the two stations every 15 min over 1 year. By identifying periods when effluent discharges to the river were halted for maintenance or operational testing—a relatively common occurrence—we were able to distinguish between the change in  $\text{NO}_3^-$  concentration associated with inputs of  $\text{NH}_4^+$ -enriched effluent from that occurring under effluent-free conditions. Assuming that all processes affecting the concentration of  $\text{NO}_3^-$  in the water column except nitrification of wastewater-derived  $\text{NH}_4^+$  were the same in the presence versus the absence of effluent permitted us to estimate nitrification rates of  $\text{NH}_4^+$  from effluent. This new approach of using continuous data from paired stations to quantify rates of change in  $\text{NO}_3^-$  concentration ( $\Delta\text{NO}_3^-$ ) and estimate nitrification rates has broad applications, even in dynamic areas such as tidal rivers and estuaries.

## 2. Materials and Methods

### 2.1. Site Description

The Sacramento-San Joaquin River Delta (Delta), which comprises the landward region of the larger San Francisco Estuary, is located in Northern California. The Sacramento River is the primary source of both water and nitrogen to the tidal reaches of the Delta, with treated wastewater effluent inputs from the Sacramento Regional WWTP contributing ~90% of the  $\text{NH}_4^+$  to the Sacramento River (Jassby, 2008; Saleh & Domagalski, 2015). This study focused on the lower stretch of the river between Freeport (FPT) and Walnut Grove (WGA), a channelized freshwater section of the river about 150–200 m wide and 4–10 m deep (supporting information Figure S1). The banks of the river are steep, rock-leveed, and support little to no vegetation. Flows along this river are highly variable both seasonally and interannually, as determined by a combination of storm events, reservoir releases, agricultural releases and withdrawals, and tidal effects. Although this stretch of the river is far enough upstream that there is essentially no mixing of Sacramento River water with downstream water sources, tidal effects cause daily fluctuations in flow and during periods of low flow (e.g., summer months during drought years) semidiurnal tides propagating from the estuary can reverse flows as far upstream as Freeport even as the net flow continues to be seaward. The 2014 water year (1 October 2013 to 30 September 2014), during which this study took place, was one of the driest water years on record for this region.

Effluent from the regional WWTP, which serves ~1.4 million residential, commercial, and industrial customers, enters the river just downstream of the Freeport Station (Figure 1 and supporting information Figure S1). Effluent outflow data (hourly averages), and treated effluent water quality data (24 h composite and discrete samples) were provided by the WWTP. Because of regulatory requirements that limit effluent to less than 6.7% of the total river volume, daily effluent discharge from the WWTP is a function of both the amount of water entering the treatment facility and river discharge. In practice, WWTP discharge to the river is halted when river discharge falls below 36.8  $\text{m}^3/\text{s}$ . Typically effluent inputs contribute 1–3% of the river volume (O'Donnell, 2014).

Currently, WWTP operations do not include nitrification or denitrification, thus the predominant form of nitrogen in the effluent is  $\text{NH}_4^+$ . During the study period, effluent  $\text{NH}_4^+$  concentrations ranged between 1800 and 2500  $\mu\text{M}$ . Thus, while  $\text{NH}_4^+$  concentrations in the river upstream of the WWTP were typically below 3  $\mu\text{M}$ , following effluent addition, concentrations increase to 15–100  $\mu\text{M}$  (Foe et al., 2010; Kratzer et al., 2011). Nitrate concentrations in treated effluent released to the river during the study period were below the WWTP's reported detection limit (<7  $\mu\text{M}$ ), which following dilution in the river corresponds to, at most, increases in river concentrations of less than 0.3  $\mu\text{M}$ .

## 2.2. High Frequency Data Collection

In situ water quality data were collected at the USGS stations at Freeport (FPT; USGS 11447650), just upstream (0.18 km) of the WWTP's discharge pipe, and Walnut Grove (WGA; USGS 11447890) 29.4 km downstream. Between the FPT and WGA stations, there were no significant inflows to the Sacramento River. The stations report velocity, discharge, and water quality data including temperature, turbidity, specific conductance, dissolved oxygen, pH, dissolved organic matter fluorescence (fDOM), chlorophyll *a* fluorescence (fCHL), and  $\text{NO}_3^-$  concentration every 15 min (<http://waterdata.usgs.gov/usa/nwis>).  $\text{NO}_3^-$  concentrations were measured using automated submersible ultra-violet nitrate analyzers (SUNA, Version 2; Satlantic, NS, Canada), which measures both  $\text{NO}_3^-$  and  $\text{NO}_2^-$ . Manufacturer stated precision for these 10 mm path length instruments is 0.3  $\mu\text{M}$  (0.004 mg  $\text{N L}^{-1}$ ) and accuracy is 2  $\mu\text{M}$  (0.028 mg  $\text{N L}^{-1}$ ). Both instruments were deployed with autonomous wipers, serviced approximately monthly, and the data collected and processed according to the methods described in Pellerin et al. (2013). Prior to deployment, sensor calibration was verified using organic-free DI water and two standards (71.4 and 714.3  $\mu\text{M}$ ). Each 15 min measurement represents the median value of a 30 s burst (Pellerin et al., 2013). Dark counts and the root-mean-square error (RMSE; less than 0.001) between the measured and the fitted absorbance were reported in real time for every measurement made in the field to detect lamp degradation. There was a strong relationship between in situ  $\text{NO}_3^-$  concentration data and discrete samples analyzed by standard laboratory methods ( $R^2 = 0.94$ ; supporting information Figure S2), and these data verified that the two sensors were calibrated similarly. Prior studies have confirmed the river is well mixed with regard to dissolved constituents (Kraus et al., 2017b; Parker et al., 2012).

## 2.3. Effluent Discharge Holds

Operation of the WWTP resulted in over 25 instances between October 2013 and September 2014 when effluent discharge to the river was halted for 7–31 h (O'Donnell, 2014). In addition, on 25 October 2013 and 1 June 2014, effluent releases were interrupted for ~20 h as part of river-scale nutrient manipulation experiments that explicitly compared riverine conditions in the presence and absence of effluent; these holds each resulted in a ~15 km stretch of river that was free of effluent from Sacramento's WWTP (Kraus et al., 2017b). Because there is little dispersive mixing along this river reach, most of these effluent holds were readily recognizable as the effluent-free parcel of water that passed the downstream WGA station, resulting in rapid simultaneous decreases in conductivity, fDOM and  $\text{NO}_3^-$  compared to water that contained effluent (Figure 2). In total, we identified 13 periods when water passing the WGA station was unambiguously effluent free. This allowed us to discriminate between water parcels containing effluent (+EFF) or not containing effluent (−EFF). Comparing  $\text{NO}_3^-$  concentrations at WGA under +EFF versus −EFF conditions allowed us to assess the fraction of  $\text{NO}_3^-$  attributable to effluent inputs.

## 2.4. Travel Time Calculations

To relate data collected for a given water parcel at Freeport (FPT) to data collected for that same water parcel at Walnut Grove (WGA), we needed to determine the travel time,  $T$ , between stations, accounting for the continuous change in parcel velocity during transit.

We calculated travel time iteratively as follows. For each 15 min time step ( $n$ ) the distance a water parcel located  $d$  km downstream of FPT traveled in a given interval was given by the product of the parcel velocity at that particular location and the 15 min time interval, with the cumulative distance traveled ( $d$ ) over  $n$  time interval calculated as

$$d_n(\text{km}) = \sum_0^n v_n^d \times t \quad (1)$$

With  $v_n^d$  the velocity of the parcel at distance  $d$  from WGA for iteration  $n$ , and  $t$  the 15 min time step. We assumed  $v_n^d$  along the stretch of river between FPT and WGA was a linear function of the velocities measured at FPT ( $v^{\text{FPT}}$ ) and WGA ( $v^{\text{WGA}}$ ) at time interval  $n$ :

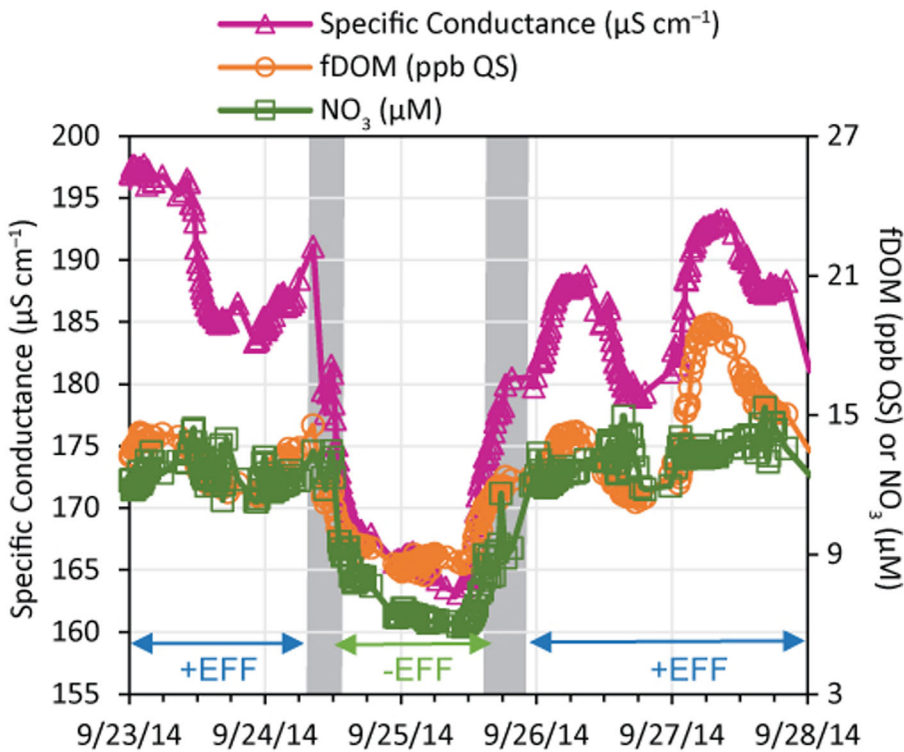


**Figure 2.** High frequency (15 min) data for specific conductance, fluorescence of dissolved organic matter (fDOM), and nitrate concentration ( $\text{NO}_3^-$ ) at Walnut Grove showing the passage of an effluent-free parcel of water. Vertical gray bars indicate the transition zone between water parcels identified as containing effluent (+EFF) and free of effluent (-EFF). Note that river velocity is strongly affected by the tidal forcings thus changes over time are not directly reflective of river length.

$$v_n^d (\text{km min}^{-1}) = \left[ 1 - \frac{d_{n-1}}{29.4} \right] v_n^{FPT} + \left[ \frac{d_{n-1}}{29.4} \right] v_n^{WGA} \quad (2)$$

where 29.4 km is the distance between FPT and WGA. Substituting equation (2) into (1) gives

$$d_n (\text{km}) = \sum_0^n \left( \left[ 1 - \frac{d_{n-1}}{29.4} \right] v_n^{FPT} + \left[ \frac{d_{n-1}}{29.4} \right] v_n^{WGA} \right) t \quad (3)$$

which is the total distance a parcel traveled from Freeport after  $n$  time steps. A solution is achieved when  $d_n$  is equal to or slightly greater than 29.4 km. The total time ( $T$ ) for each water parcel to travel from FPT to WGA is then given as

$$T(\text{min}) = n \times t \quad (4)$$

The effluent discharge holds—which created effluent-free sections of the river with notably different water quality (Figure 2)—provided a means to validate the travel time model and estimate the associated uncertainty. The measured time water took to transit between the WWTP and WGA was calculated as the difference between the start and end times of the effluent holds as recorded by the WWTP, and the times the corresponding diagnostic fronts in conductivity, fDOM, and  $\text{NO}_3^-$  were observed at WGA. Measured travel times compared well with the modeled travel times ( $R^2 = 0.92$ ;  $n = 52$ ; supporting information Figure S3).

### 2.5. Changes in $\text{NO}_3^-$ Concentration

The change in  $\text{NO}_3^-$  concentration ( $\Delta \text{NO}_3^-$ ,  $\mu\text{M}$ ) between the two monitoring stations was calculated for each 15 min measurement as the difference between the  $\text{NO}_3^-$  concentration measured at FPT at time  $t$ , and the concentration measured as the water parcel passed WGA at time  $t$  plus the calculated travel time  $T$ :

$$\Delta NO_3 (\mu M) = [NO_3]_{WGA}^{t+T} - [NO_3]_{FPT}^t \quad (5)$$

Dividing  $\Delta NO_3$  by travel time provides the rate of change in  $NO_3^-$  per day:

$$R_{\Delta NO_3} (\mu M \text{ d}^{-1}) = \frac{\Delta NO_3}{T} \quad (6)$$

These calculations were also made for the 13 effluent holds by visually inspecting the WGA  $NO_3^-$  concentration data during the time period the travel time model predicted the effluent-free parcels of water were passing that station to identify values unambiguously absent of effluent inputs (Figure 2). The average  $NO_3^-$  concentration immediately prior and subsequent to the -EFF conditions was taken to be representative of the river under normal +EFF conditions. The average associated  $NO_3^-$  concentration at Freeport and average travel times encompassing an entire hold period (encompassing both +EFF and -EFF conditions) were used to calculate the change in  $NO_3^-$  concentration ( $\Delta NO_3$ ) and rate of change under +EFF and -EFF conditions ( $R_{\Delta NO_3}^{+EFF}$  and  $R_{\Delta NO_3}^{-EFF}$ , respectively).

Because the river normally is under +EFF conditions and only occasionally experiences -EFF conditions, we had continuous high frequency data for  $R_{\Delta NO_3}^{+EFF}$  but only intermittent data for  $R_{\Delta NO_3}^{-EFF}$ . We thus applied a linear interpolation to the  $R_{\Delta NO_3}^{-EFF}$  values determined for the 13 effluent holds periods. Because there was a significant gap in measured  $R_{\Delta NO_3}^{-EFF}$  between January and June (Figure 3b), encompassing the period when the  $\Delta NO_3^-$  rose markedly, we used the relationship between  $\Delta NO_3$  and temperature to extend the period of low  $R_{\Delta NO_3}^{-EFF}$  values observed during the colder months (October–January) to mid-April when temperatures rose above 15°C, and then linearly interpolated the data point-to-point thereafter (see sections 3 and 4 for details).

## 2.6. Nitrification

Following our conceptual model shown in Figure 1, we took the difference between the  $R_{\Delta NO_3}^{+EFF}$  and the  $R_{\Delta NO_3}^{-EFF}$  to estimate the nitrification rate of effluent-derived  $NH_4^+$  ( $R_{Nitrif-E}$ ):

$$R_{Nitrif-E} (\mu M \text{ d}^{-1}) = R_{\Delta NO_3}^{+EFF} - R_{\Delta NO_3}^{-EFF} = \frac{NO_3^{+EFF}_{WGA} - NO_3^{-EFF}_{WGA}}{T} \quad (7)$$

This calculation assumes that all processes affecting the concentration of  $NO_3^-$  in the water column, except nitrification of wastewater-derived  $NH_4^+$ , were the same in the presence versus the absence of effluent additions (see below a discussion of these assumptions). We calculated  $R_{Nitrif-E}$  for the 13 effluent hold periods and also for each 15 min time step using the measured  $R_{\Delta NO_3}^{+EFF}$  and the interpolated  $R_{\Delta NO_3}^{-EFF}$  data. Note that for the 10 April 2014 effluent hold, the FPT station SUNA was not functioning, but we were still able to calculate  $R_{Nitrif-E}$  by taking the difference in  $NO_3^-$  concentration between +EFF and -EFF conditions at WGA (equation (7)).

## 2.7. Data Treatment and Statistical Analysis

Because tidal reversals at FPT can transport water containing effluent additions from the WWTP upstream past the monitoring station, we excluded periods when Sacramento River discharge at FPT was  $<100 \text{ m}^3 \text{ s}^{-1}$  (Figure 1). Also, due to the high uncertainty in travel times and  $NO_3^-$  concentration values associated with high flow storm events when conditions were rapidly changing, we excluded data associated with travel times  $<1.3$  days from calculations of  $\Delta NO_3^-$  concentration,  $R_{\Delta NO_3}$  and  $R_{Nitrif-E}$ . We excluded WGA  $NO_3^-$  data identified as periods of transition between -EFF and +EFF conditions from analysis (Figure 2). For each of the 13 effluent hold periods, the average and standard deviation of the  $NO_3^-$  concentrations associated with -EFF and +EFF parcels passing by WGA (Figure 2), and the associated concentrations when those parcels previously passed FPT, were calculated. These standard errors were propagated through the hold data  $\Delta NO_3^-$ ,  $R_{\Delta NO_3}^{+EFF}$ , and  $R_{\Delta NO_3}^{-EFF}$  calculations. Where indicated, 15 min time series data were tidally filtered (Godin, 1972). Single and multiple linear regressions were calculated using JMP software version 12.0 (SAS Institute, Inc., 2015). Trends were considered significant when  $p$  values were  $<0.001$ .

## 3. Results

### 3.1. Discharge, Travel Time, and Water Quality

Tidally averaged base flows measured at Freeport ranged from  $150$  to  $300 \text{ m}^3 \text{ s}^{-1}$ , while during storm events discharge increased above  $500 \text{ m}^3 \text{ s}^{-1}$  (Figure 3a). Modeled travel times between FPT and WGA

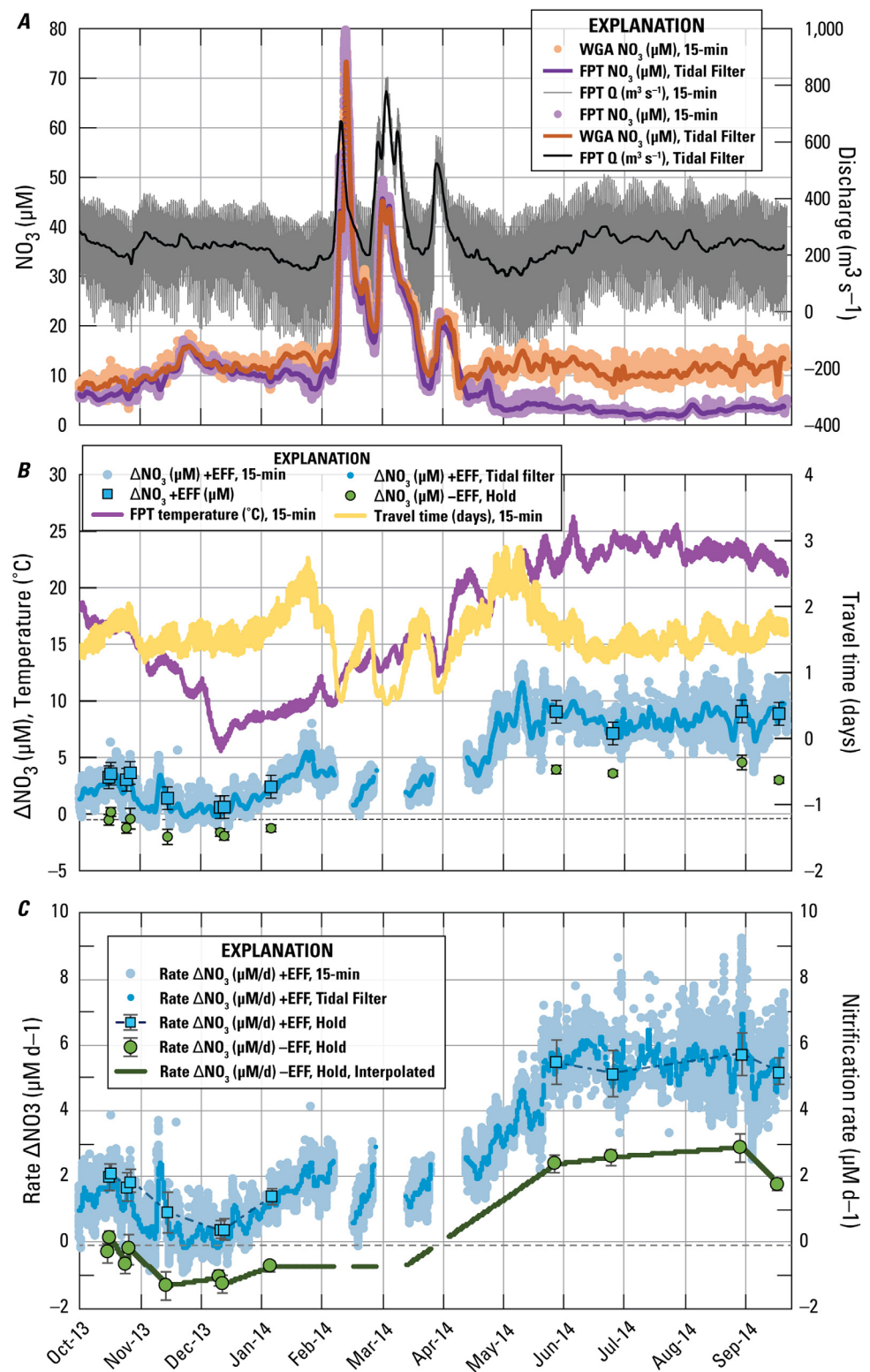


**Figure 3.** Time series showing (a) nitrate ( $\text{NO}_3$ ) concentrations at Freeport (FPT) and Walnut Grove (WGA) plotted along with instantaneous (15 min) and tidally filtered discharge at FPT, (b) change in  $\text{NO}_3$  concentration ( $\Delta\text{NO}_3$ ) during travel between FPT and WGA in the presence of effluent (+EFF) and absence of effluent (-EFF) plotted along with travel time and water temperature, (c) the rate of change in  $\text{NO}_3$  concentration measured under +EFF ( $R_{\Delta\text{NO}_3}^{+EFF}$ ) and -EFF ( $R_{\Delta\text{NO}_3}^{-EFF}$ ) conditions. Data associated with the effluent hold periods are referred to as "Hold" data.

ranged from 0.5 to 3 days but were most frequently between 1.3 and 2 days (Figure 3b). Travel times of less than 1.3 days were associated with storm events and subsequent higher flows in February–April.

Water temperatures were cooler in the winter months (November–February,  $<15^{\circ}\text{C}$ ) and increased rapidly in March–May to reach temperatures between 22 and  $26^{\circ}\text{C}$  in June–September. Although turbidities reached over 100 FNU's during storm events, for the rest of the study period they fluctuated daily from  $\sim 2$  to 15 FNU's, equivalent to suspended sediment concentrations of about  $10\text{--}30\text{ mg L}^{-1}$ . Specific conductance ranged between 115 and  $265\text{ }\mu\text{S cm}^{-1}$  and was generally higher in the winter months except during high flow events. Dissolved oxygen saturation fluctuated between 75 and 115% and was typically about 5% lower at WGA compared to FPT. Temperature, turbidity, specific conductance and dissolved oxygen data for the study period are provided in supporting information Figure S4.

### 3.2. Nitrate Concentrations

Nitrate concentrations at FPT generally ranged from  $\sim 2$  to  $12\text{ }\mu\text{M}$  during nonstorm periods, and increased rapidly during storm events to concentrations as high as  $80\text{ }\mu\text{M}$  (Figure 3a).  $\text{NO}_3^-$  concentrations at FPT were particularly low ( $2\text{--}6\text{ }\mu\text{M}$ ) during the warmer summer months (May–August). This pattern is consistent with prior observations (Foe et al., 2010; Kratzer et al., 2011; Schlegel et al., 2016).

During normal conditions when effluent was released into the river (+EFF conditions),  $\text{NO}_3^-$  concentrations typically increased as water transited between FPT and WGA, with the increase larger in summer than winter (Figure 3b). Rates of change in  $\text{NO}_3^-$  concentration,  $R_{\Delta\text{NO}_3}^{+EFF}$ , were variable in the fall and winter (October–February) ranging from near zero to  $\sim 2.0\text{ }\mu\text{M d}^{-1}$ , increased during the spring (March–May), and stabilized in the summer months (June–September) near  $\sim 5.5\text{ }\mu\text{M d}^{-1}$  (Figure 3c and Table 1).

In the absence of effluent (−EFF),  $\text{NO}_3^-$  concentrations decreased  $\sim 0.5\text{--}2.0\text{ }\mu\text{M}$  as water transited between the stations during the fall and winter months but increased  $\sim 4\text{ }\mu\text{M}$  in the summer months (Table 1 and Figure 3b). Consequently,  $R_{\Delta\text{NO}_3}^{-EFF}$  in the winter ranged from  $-1.3$  to  $0.1\text{ }\mu\text{M d}^{-1}$  compared to a range of  $1.8\text{--}2.9\text{ }\mu\text{M d}^{-1}$  in the summer (Table 1 and Figure 3c).

As mentioned above, during winter storm events we found high uncertainty in calculated  $\Delta\text{NO}_3^-$ , owing to the rapid changes in  $\text{NO}_3^-$  concentration and travel times (Figure 3). We thus did not attempt to calculate

**Table 1**

Nitrate ( $\text{NO}_3^-$ ) Concentration Data at Freeport (FPT) and Walnut Grove (WGA) During the 13 Periods of Identifiable Effluent Holds Along With Water Temperature, Travel Time, Change in  $\text{NO}_3^-$  Concentration ( $\Delta\text{NO}_3$ ,  $\mu\text{M}$ ) and Rate of  $\text{NO}_3^-$  Change (Rate  $\Delta\text{NO}_3$ ,  $\mu\text{M d}^{-1}$ ) in the Presence of Effluent (+EFF) and the Absence of Effluent (−EFF), and Nitrification Rates of Effluent-Derived Ammonium ( $R_{\text{Nitrific\_E}}$ ) Estimated by Difference

Date	10/16/13	10/17/13	10/25/13	10/27/13	11/15/13	12/12/13	12/14/13	1/7/14	4/10/14	6/2/14	7/1/14	9/5/14	9/24/14
Temperature, WGA (°C)	17	17	17	17	14	6	7	9	18	22	24	23	22
Travel time FPT to WGA (days)	1.6	1.7	1.8	1.9	1.5	1.5	1.5	1.7	1.4	1.6	1.4	1.6	1.7
Nitrate concentrations ( $\mu\text{M}$ )													
FPT	5.9	6.0	6.2	5.2	11.0	11.8	11.6	8.6	NA	3.5	2.8	3.5	3.4
WGA-EFF	5.4	6.2	5.0	4.8	9.0	10.1	9.7	7.4	16.4	7.4	6.4	8.1	6.4
WGA+EFF	9.2	9.6	9.3	8.8	12.4	12.4	12.2	11.1	20.5	12.5	10.0	12.6	12.3
Nitrate at WGA attributed to noneffluent sources and effluent sources (%)													
% $\text{NO}_3$ ambient	59	65	54	54	72	82	79	67	80	59	64	64	52
% $\text{NO}_3$ attributed to effluent	41	35	46	46	28	18	21	33	20	41	36	36	48
Change in nitrate between FPT and WGA ( $\mu\text{M}$ )													
$\Delta\text{NO}_3$ -EFF	-0.5	0.2	-1.2	-0.4	-2.0	-1.6	-1.9	-1.3	NA	3.9	3.6	4.6	3.0
$\Delta\text{NO}_3$ +EFF	3.3	3.6	3.0	3.6	1.4	0.6	0.6	2.4	NA	9.0	7.1	9.1	8.9
Change attributed to effluent	<b>3.8</b>	<b>3.4</b>	<b>4.3</b>	<b>4.1</b>	<b>3.4</b>	<b>2.2</b>	<b>2.5</b>	<b>3.7</b>	<b>4.2</b>	<b>5.1</b>	<b>3.5</b>	<b>4.5</b>	<b>5.9</b>
Rate of change in nitrate between FPT and WGA ( $\mu\text{M d}^{-1}$ )													
Rate $\Delta\text{NO}_3$ -EFF	-0.3	0.1	-0.7	-0.2	-1.3	-1.1	-1.3	-0.7	NA	2.4	2.6	2.9	1.8
Rate $\Delta\text{NO}_3$ +EFF	2.0	2.1	1.7	1.9	0.9	0.4	0.4	1.4	NA	5.5	5.1	5.7	5.2
Nitrification rate ( $R_{\text{Nitrific\_E}}$ )	<b>2.3</b>	<b>2.0</b>	<b>2.4</b>	<b>2.1</b>	<b>2.2</b>	<b>1.5</b>	<b>1.7</b>	<b>2.1</b>	<b>3.1</b>	<b>3.1</b>	<b>2.5</b>	<b>2.9</b>	<b>3.4</b>

Note. NA, not available.

$R_{\Delta\text{NO}_3}$  for these periods ( $T < 1.3$  days). However, because water temperatures were low (10–15°C), and travel times were short, we expect little change in  $\text{NO}_3^-$  concentration occurred between the stations during these periods.

### 3.3. Nitrification Rates

Comparing changes in the  $\text{NO}_3^-$  pool associated with the effluent hold +EFF and -EFF conditions (equation (7)) allowed us to estimate nitrification rates. We started by examining the  $R_{\text{Nitrif},E}$  values associated with 13 instances when effluent discharge was held for a sufficient period of time to permit unambiguous identification of effluent-free conditions.  $R_{\text{Nitrif},E}$  values calculated for these periods—nine instances from November 2013 through January 2014 (winter) and five instances from April 2014 through September 2014 (summer).  $R_{\text{Nitrif},E}$  values were lower in the winter at about  $\sim 2.0 \mu\text{M d}^{-1}$  and higher in the summer at  $\sim 3.0 \mu\text{M d}^{-1}$  (Table 1;  $t$  test,  $p$ -value < 0.001,  $F$ -ratio = 120.8).

We also estimated  $R_{\text{Nitrif},E}$  values for each 15 min time step using the interpolated  $R_{\Delta\text{NO}_3}^{-\text{EFF}}$  data and measured  $R_{\Delta\text{NO}_3}^{+\text{EFF}}$  data. The high frequency time series of  $R_{\text{Nitrif},E}$  calculated in this way contained considerable variability (Figure 4). We believe this variability is primarily the result of imprecision in the travel time calculations (see supporting information Figure S3) and the challenge of accurately linking parcels of water passing the upstream station with the downstream station in this tidal system. In particular, the estimated high frequency  $R_{\text{Nitrif},E}$  values for February–May when storm events caused rapid fluctuations in discharge were particularly variable, and did not align well with the one effluent hold rate measured in April (Figure 4). This points to the need to obtain more validation data (i.e., planned effluent holds). There is also some error associated with the  $\text{NO}_3^-$  measurement itself, which can make it challenging to detect small changes in concentration. Positioning another station farther downstream would lengthen the travel time a parcel could be tracked, and allow for a greater change in  $\text{NO}_3^-$  to be measured which would lower the uncertainty associated with these estimates. Despite these uncertainties, estimated values in the fall and winter were generally relatively low ( $\sim 1.0$ – $2.5 \mu\text{M d}^{-1}$ ) and they rose in the spring and summer to values of  $\sim 2.0$ – $4 \mu\text{M d}^{-1}$ . Furthermore, the power of the replication inherent in using high frequency data to make this calculation is that we can apply smoothing approaches, like a tidal filter (Figures 3 and 4), and gain information about temporal trends that would not be feasible using traditional approaches.

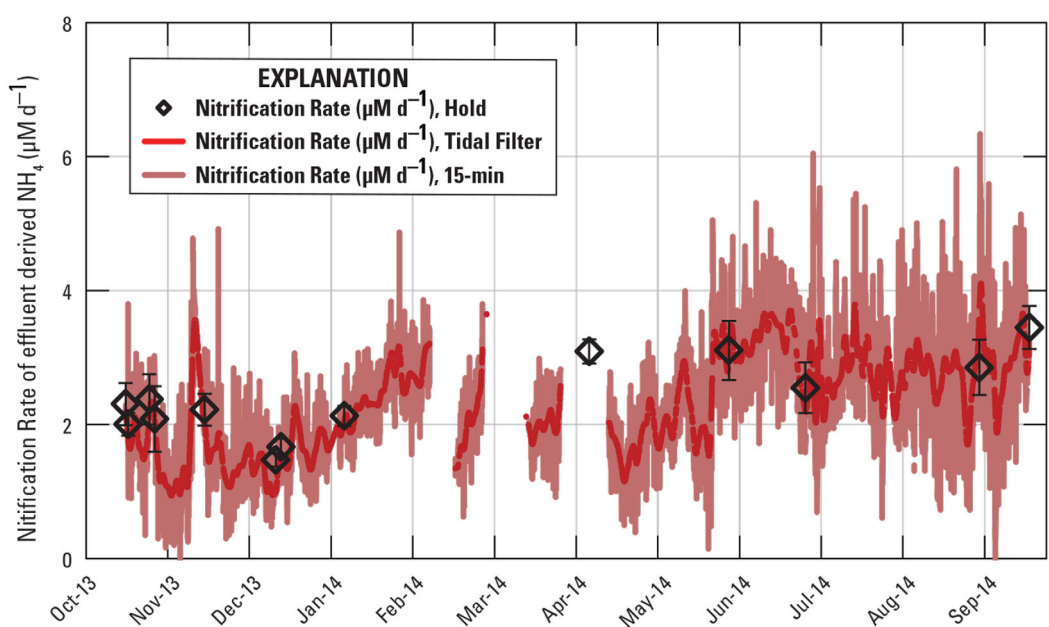


**Figure 4.** Time series showing nitrification rates of effluent-derived ammonium ( $R_{\text{Nitrif},E}$ ). Data associated with the effluent hold periods are referred to as “Hold” data.

### 3.4. Regression Analyses

To explore environmental factors related to the  $\text{NO}_3^-$  concentration in the river under normal +EFF operational conditions, we ran single linear regressions between the  $R_{\Delta\text{NO}_3}^{+EFF}$  versus water temperature. There was a strong significant correlation between the  $R_{\Delta\text{NO}_3}^{+EFF}$  and water temperature ( $R^2 = 0.73$ ), particularly for the warmer summer months ( $>15.0^\circ\text{C}$ ;  $R^2 = 0.81$ ; Figure 5a). In the colder winter months ( $<15.0^\circ\text{C}$ )  $R_{\Delta\text{NO}_3}^{+EFF}$  values were close to zero and not significantly correlated to temperature (Figure 5a). We found only weak correlations between tidally filtered  $R_{\Delta\text{NO}_3}^{+EFF}$  with travel time ( $R^2 = 0.01$ ), turbidity ( $R^2 = 0.01$ ), specific conductivity ( $R^2 = 0.20$ ), dissolved oxygen ( $R^2 = 0.01$ ), and pH ( $R^2 = 0.06$ ). Although all of these factors were significant in a stepwise multiple regression model at the 0.001 level, the predictive ability of this more complex model provided little additional benefit ( $R^2 = 0.81$ ) compared to temperature alone.

We also ran correlations on the data associated with the 13 effluent hold periods (Table 1). During the warmer months ( $>15^\circ\text{C}$ ), temperature was found to be significantly correlated with  $R_{\Delta\text{NO}_3}^{+EFF}$  ( $R^2 = 0.93$ ) and  $R_{\Delta\text{NO}_3}^{-EFF}$  ( $R^2 = 0.81$ ) (Figure 6). For  $R_{\Delta\text{NO}_3}^{+EFF}$ , there was good agreement between the  $>15^\circ\text{C}$  temperature

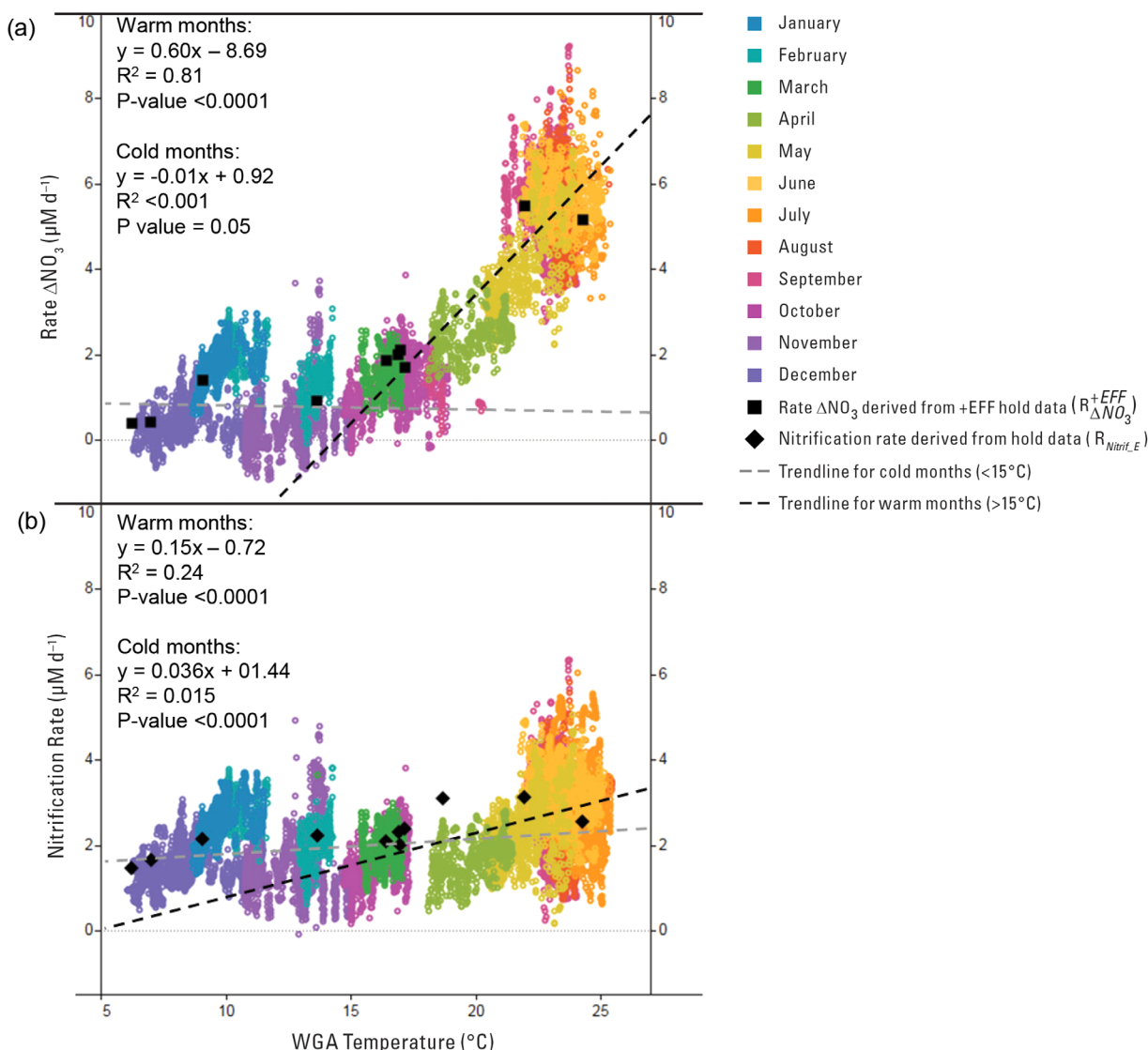


**Figure 5.** Relationship between water temperature at Walnut Grove (WGA) and (a) the rate of change in  $\text{NO}_3^-$  concentration under +EFF conditions ( $R_{\Delta\text{NO}_3}^{+EFF}$ ) and (b) the nitrification rate ( $R_{\text{Nitrif}}$ ). Black symbols depict data calculated during the effluent hold periods while symbols color coded by month depict the high frequency data. Regression lines are fit separately to data associate with temperature  $>15^\circ\text{C}$  (warm months) and  $<15^\circ\text{C}$  (cold months).

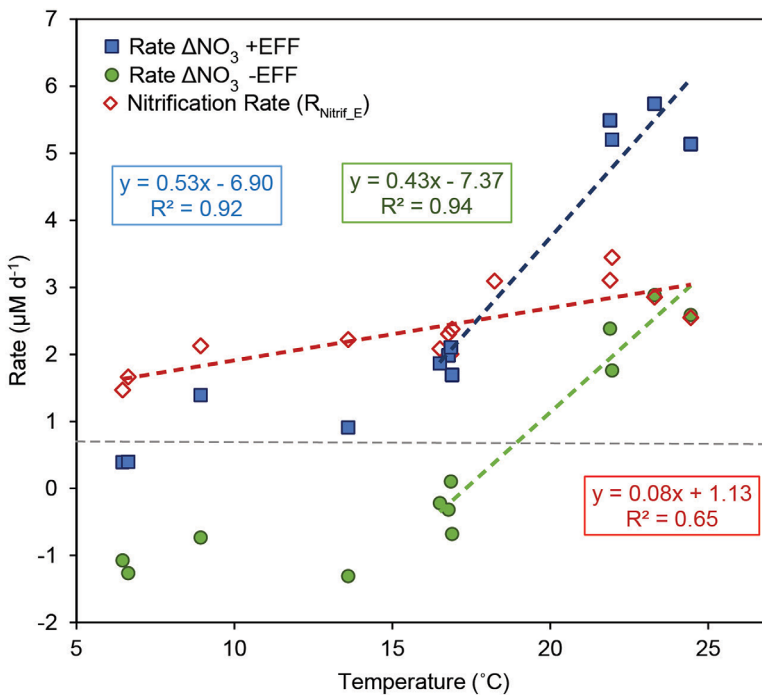


**Figure 6.** The relationship between temperature and the rate of change in nitrate concentration in the presence and absence of effluent ( $R_{\Delta\text{NO}_3}^{+EFF}$  and  $R_{\Delta\text{NO}_3}^{-EFF}$ , respectively), and the rate of nitrification ( $R_{\text{Nitrif}}$ ). The regression lines for  $R_{\Delta\text{NO}_3}^{+EFF}$  and  $R_{\Delta\text{NO}_3}^{-EFF}$  are only fit to data where temperature was  $>15^{\circ}\text{C}$ , while for  $R_{\text{Nitrif}}$  they include all data.

relationship developed using the high frequency data ( $R_{\Delta\text{NO}_3}^{+EFF} = 0.60 \times \text{Temp} - 8.69$ ) and the hold data ( $R_{\Delta\text{NO}_3}^{+EFF} = 0.50 \times \text{Temp} - 6.31$ ).

Temperature was also found to be significantly correlated with  $R_{\text{Nitrif},E}$  calculated for the hold data, however the predictive ability was lower ( $R^2 = 0.65$  for all data,  $R^2 = 0.41$  for  $>15^{\circ}\text{C}$ ), and the slope of the relationship was less steep than for rates of change measured for the total  $\text{NO}_3^-$  pool (Figure 6). For estimated high frequency  $R_{\text{Nitrif},E}$  values, the relationship with temperature was significant but weaker ( $R^2 = 0.24$  for data  $>15^{\circ}\text{C}$ , Figure 5b), however there was also good agreement between  $R_{\text{Nitrif},E}$  and the  $>15^{\circ}\text{C}$  temperature relationship developed using the high frequency data ( $R_{\text{Nitrif},E} = 0.15 \times \text{Temp} - 0.72$ ) and the  $R_{\text{Nitrif},E}$  values associated with the 13 effluent holds ( $R_{\text{Nitrif},E} = 0.09 \times \text{Temp} + 0.92$ ).

#### 4. Discussion

Like many other large temperate rivers, in the absence of anthropogenic inputs the Sacramento River typically has low concentrations of  $\text{NO}_3^-$  ( $<15 \mu\text{M}$ ), except during storm events when hydrologic connectivity to upstream terrestrial sources leads to elevated concentrations (Downing et al., 2017; Kratzer et al., 2011). While the total annual nitrogen loads exported from the Sacramento River to the downstream estuary is predominantly attributed to diffuse upstream sources (Saleh & Domagalski, 2015), those inputs typically occur during high flow storm events when constituents in the water column rapidly transit the ecosystem (i.e., short travel times). In the absence of higher upstream  $\text{NO}_3^-$  concentrations, the high and consistent nitrogen loading from the Sacramento Regional WWTP is the primary source of dissolved inorganic nitrogen (DIN) to the Sacramento River and northern Delta, contributed predominantly as  $\text{NH}_4^+$  that can be converted to  $\text{NO}_3^-$  via nitrification (Jassby, 2008; Novick et al., 2015). Under these normal operational conditions, when effluent high in  $\text{NH}_4^+$  is continuously discharged to the river, progressive increases in  $\text{NO}_3^-$  concentration are observed as water travels downstream of the WWTP; analogous  $\text{NO}_3^-$  concentration increases are not observed upstream of the WWTP (Foe et al., 2010; Kraus et al., 2017b; Parker et al., 2012), indicating that the increases below the WWTP are associated with the effluent inputs. Given that there are no substantive inputs into the Sacramento River downstream of the WWTP, the most apparent explanation is that the observed progressive downstream increase in  $\text{NO}_3^-$  concentration results from nitrification of effluent-

derived  $\text{NH}_4^+$ . Changes in the isotopic composition of the  $\text{NO}_3^-$  and  $\text{NH}_4^+$  pool support this notion (Kendall et al., 2015; Novick et al., 2015). As we discuss below, however, the situation is somewhat more complex because increases in the  $\text{NO}_3^-$  pool were observed both in the presence and absence of effluent, even though groundwater inputs of nitrate are thought to be insignificant in this stretch of the Sacramento River (Faunt, 2009).

#### 4.1. Nitrification

In the presence of effluent, greater increases in  $\text{NO}_3^-$  were observed during transit between the two stations compared to the absence of effluent, indicating that nitrification of effluent-derived  $\text{NH}_4^+$  is responsible for a significant fraction of downstream  $\text{NO}_3^-$  concentrations (Figures 1 and 3 and Table 1). Nitrification rates associated with effluent-derived ammonium measured for the 13 effluent holds ( $R_{\text{Nitrif,E}}$ ) ranged from 1.5 to  $3.5 \mu\text{M d}^{-1}$ , with individual 15 min values ranging from 0.3 to  $4.0 \mu\text{M d}^{-1}$ . Both showed strong seasonal dependency (Figure 5). Based on these rates, after  $\sim 2$  days of travel downstream of the WWTP, nitrification of effluent-derived  $\text{NH}_4^+$  accounted for up to 50% of the  $\text{NO}_3^-$  in the river at WGA (Table 1 and supporting information Figure S7).

Finding appropriate data to validate the rates estimated here is difficult given that this is the first study of its kind. The most direct comparison is from the Lagrangian sampling campaign conducted along the same stretch of the Sacramento River in association with the October 2013 and June 2014 effluent holds (Kraus et al., 2017b). In that study, +EFF and -EFF parcels of water were tracked and sampled by boat as they traveled 50 km downstream of the WWTP over a period of  $\sim 3.5$  days. Based on those data, nitrification rates of effluent-derived  $\text{NH}_4^+$  were on average  $2.2 \pm 0.9 \mu\text{M d}^{-1}$  in October and  $2.9 \pm 0.6 \mu\text{M d}^{-1}$  in June (supporting information Table S1), very close to the winter rates of  $2.0 \pm 0.3 \mu\text{M d}^{-1}$  and summer rates of  $3.0 \pm 0.3 \mu\text{M d}^{-1}$  estimated from the holds identified at the WGA station in this study (Figure 4 and Table 1). Using a mass balance approach Parker et al. (2012) estimated nitrification rates over a larger stretch of the Sacramento River and extending into the estuary, by taking the difference in mean  $\text{NO}_3^-$  concentrations between a site just upstream of WGA and another about 60 km farther downstream and dividing by an estimated travel time of 4.6 days. The resulting estimated rates were  $4.0\text{--}6.4 \mu\text{M d}^{-1}$  in March and April 2009, which are similar to what we measured for the rate of change in  $\text{NO}_3^-$  concentration in summer ( $5.4 \pm 0.3 \mu\text{M d}^{-1}$ ; Table 1), but higher than what we attribute specifically to effluent-associated nitrification ( $\sim 3 \mu\text{M d}^{-1}$ ; Table 1).

There are few other direct validation data available against which we can compare the magnitude and variability of the rates determined here, owing to the fact that measurement of nitrification rates using conventional methods is difficult and labor intensive. Therefore, comparative values are only available from a relatively small number of locations, for a small number of samples and for only relatively short spans of time. Nitrification rates measured in this study of  $1.5\text{--}3.4 \mu\text{M d}^{-1}$  easily fall within the wide range of values reported in a recent review (Damashek et al., 2016). They are comparable to those measured in freshwater systems like the Mississippi River (Carini et al., 2010; up to  $3.5 \mu\text{M d}^{-1}$ ), Tamar estuary (Owens, 1986; up to  $4.0 \mu\text{M d}^{-1}$ ), Rhone River (Bianchi et al., 1999; up to  $4.1 \mu\text{M d}^{-1}$ ), and Chang Jian River (Hsiao et al., 2014; up to  $4.6 \mu\text{M d}^{-1}$ ), but much lower than some values reported for the Nervion River (Iriarte et al., 1998; up to  $14 \mu\text{M d}^{-1}$ ), the Pearl River (Dai et al., 2008; up to  $33 \mu\text{M d}^{-1}$ ), and the Scheldt estuary (Andersson et al., 2006; up to  $150 \mu\text{M d}^{-1}$ ).

Damashek et al. (2016) used the  $^{15}\text{N}$  tracer incubation approach to measure water column (pelagic) nitrification rates in the San Francisco Bay and estuary on three dates (October 2011, December 2011, and February 2012), including one site on the Sacramento River at Rio Vista about 25 km downstream of WGA, and reported rates an order of magnitude lower ( $0.07\text{--}0.18 \mu\text{M d}^{-1}$ ) than what we measured using our in situ approach. We are unable to explain this discrepancy, but note that the rates reported by Damashek et al. (2016) represent pelagic measurements, whereas the in situ approach we used takes into account nitrification that occurs both in the water column and at the sediment-water interface, although given the depth of the Sacramento River over the experimental reach ( $\sim 4\text{--}10$  m) it seems unlikely to completely explain the difference. The sites Damashek et al. (2016) sampled were farther downstream on the Sacramento River, where tidal mixing affects salinity, temperature, dissolved oxygen concentrations, and turbidity, and in some cases  $\text{NH}_4^+$  concentrations may be limiting nitrification rates.

Although many of the papers cited above highlight the importance of temperature, availability of  $\text{NH}_4^+$ , turbidity, salinity, and the size of the nitrifying microbial community as factors affecting rates, it is difficult to assess the extent to which these factors affect nitrification rates at the landscape scale when these factors covary. Measurements based on incubations in many cases represent operationally defined *potential* nitrification rates because they are carried out under controlled conditions of temperature and light with readily available  $\text{NH}_4^+$  and oxygen, and estimates made using  $^{14}\text{C}$  instead of  $^{15}\text{N}$  tracer incubation methods may provide disparate results (Andersson et al., 2006). Additionally, because these measurements are difficult to make, they are often conducted on a single sample collected at a specific location, depth, and time, and thus typically do not capture the dynamic spatial and temporal conditions of the natural environment. For example, Damashek et al. (2016) found that even in the well-mixed downstream San Francisco Estuary nitrification rates were commonly, but not always, over 2 times greater at depth compared to surface waters, presumably due to the presence of particulate material. Other studies suggest that diel factors like light, temperature and dissolved oxygen can affect nitrification (Damashek et al., 2016; Hensley et al., 2014, 2015; Kunz et al., 2017).

The approach we used to estimate nitrification rates—comparing rates of change in  $\text{NO}_3^-$  in the presence versus the absence of effluent and attributing the difference to nitrification of effluent-derived ammonium (Figure 1 and equation (7))—contains several implicit assumptions. First, we assumed negligible influence from unknown inputs such as small agricultural dischargers, discharge from recreational boats or marinas, groundwater and others because these sources would be spatially variable and thus identified as “hot spots” in mapping campaigns conducted by previous studies (Kraus et al., 2017b). Moreover, if these inputs were the same under +EFF and -EFF conditions they would not affect our estimated change in  $\text{NO}_3^-$  attributable to effluent-derived  $\text{NH}_4^+$  (Figure 1). Second, we assumed that  $\text{NO}_3^-$  uptake rates were the same under +EFF and -EFF conditions. However, studies have shown that when  $\text{NH}_4^+$  is present phytoplankton take it up preferentially over  $\text{NO}_3^-$ , leading to negligible rates of  $\text{NO}_3^-$  uptake (Dugdale et al., 2007; Glibert et al., 2016; Parker et al., 2012). Nevertheless, reported potential  $\text{NO}_3^-$  uptake rates for the study reach made under high light conditions were only about  $0.5 \mu\text{M d}^{-1}$  greater in -EFF compared to +EFF conditions, evinced by the fact that even in the absence of effluent inputs  $\text{NH}_4^+$  concentrations increased progressively downstream of the WWTP (Kraus et al., 2017b). Thus, we believe that phytoplankton uptake in -EFF parcels, experiencing natural low light conditions, had minor effects on our nitrification estimates. However, if  $\text{NO}_3^-$  uptake was greater in the absence of effluent it would lead us to overestimate  $R_{\text{Nitrif}_E}$  by an equivalent amount (Figure 1 and equation (7)). Third, even though we did our best to exclude the mixing zone between the +EFF and -EFF parcels, dispersive mixing could have “contaminated” the -EFF parcel with +EFF water. If significant dispersive mixing occurred, it would have increased the  $\text{NO}_3^-$  and  $\text{NH}_4^+$  concentration in the -EFF parcel which would lead us to overestimate the change in  $\text{NO}_3^-$  under truly -EFF conditions, and thus underestimate  $R_{\text{Nitrif}_E}$  (Figure 1). Finally, more broadly, differences in concentrations of  $\text{NO}_3^-$ ,  $\text{NH}_4^+$  and the availability of organic carbon under +EFF and -EFF conditions can also affect nitrification, denitrification, uptake, and DNR (Bernhardt & Likens, 2002; Damashek et al., 2016; Strauss et al., 2002).

The comparison between +EFF and -EFF conditions provides estimates of nitrification of effluent-derived  $\text{NH}_4^+$  ( $R_{\text{Nitrif}_E}$ ), not whole ecosystem nitrification rates which also include nitrification of any ambient  $\text{NH}_4^+$  ( $R_{\text{Nitrif}_A}$ ; Figure 1). Although  $\text{NH}_4^+$  concentrations in the river in the absence of effluent are typically low (Kraus et al., 2017b), nitrification of the ambient  $\text{NH}_4^+$  pool is almost certainly occurring, and likely accounts for a portion of the  $\text{NO}_3^-$  that is added during transit during both +EFF and -EFF conditions. Thus, whole ecosystem nitrification rates are likely higher than our calculated  $R_{\text{Nitrif}_E}$  values.

#### 4.2. Nitrate Changes in the Absence of Effluent

One of the significant findings of this study is the extent to which the reach of the Sacramento River we studied can be a sink or source for  $\text{NO}_3^-$ , even in the absence of effluent inputs. During the colder winter months in the absence of effluent,  $\text{NO}_3^-$  concentrations typically decreased  $\sim 0.5\text{--}2.0 \mu\text{M}$  during travel between FPT and WGA, translating into negative  $R_{\Delta\text{NO}_3}^{-\text{EFF}}$  ranging between  $-0.3$  and  $-1.3 \mu\text{M d}^{-1}$  (Table 1 and Figure 3). This loss of  $\text{NO}_3^-$  reflects that processes consuming  $\text{NO}_3^-$  (e.g., uptake, denitrification) were greater than those producing  $\text{NO}_3^-$  (e.g., benthic release of  $\text{NO}_3^-$  or of  $\text{NH}_4^+$  followed by nitrification; Figure 1). In contrast, during the warmer summer months (May–September) in the absence of effluent,  $\text{NO}_3^-$  concentrations increased from  $3.0$  to  $4.6 \mu\text{M}$ , associated with  $R_{\Delta\text{NO}_3}^{-\text{EFF}}$  of  $1.8\text{--}2.9 \mu\text{M d}^{-1}$  (Table 1 and Figure 3). This reveals that during this period there are other significant sources of  $\text{NO}_3^-$  to this river reach other than nitrification of recently added effluent-derived  $\text{NH}_4^+$ , and that these sources can outweigh sinks.

Results from a Lagrangian study that tracked parcels of water traveling above and even farther downstream this reach of the Sacramento River help to constrain the possible sources of the added  $\text{NO}_3^-$  (Kraus et al., 2017b). In that study, steady increases in both water column  $\text{NO}_3^-$  and  $\text{NH}_4^+$  concentrations during transit were also observed downstream of the WWTP during periods of effluent holds. Measurement of conservative tracers associated with effluent demonstrated that this new DIN entering the water column was not due to transient storage or dispersive mixing of effluent. Because of the steady increase in DIN with distance downstream and because upstream of the WWTP DIN concentrations were low and showed no increasing trend with downstream travel, the authors attributed observed increases in DIN to benthic release of nitrogen. The increase in  $\text{NO}_3^-$  could be due to direct efflux of  $\text{NO}_3^-$  itself (from, for example, mineralization of organic matter and subsequent nitrification in the sediment, or from groundwater inputs which are not well constrained for this section of the river) or efflux of  $\text{NH}_4^+$  which is rapidly nitrified. Nutrient fluxes associated with sediment cores collected from sites downstream of this study reach have shown both net efflux and net influx of  $\text{NO}_3^-$  and  $\text{NH}_4^+$  depending on location and time of year (Cornwell et al., 2014; Kuwabara et al., 2009). Assuming these fluxes from the benthos are biologically mediated, it is likely that the observed lower flux in the winter was due to lower temperatures, which would explain the strong relationship between  $R_{\Delta\text{NO}_3^-}^{-\text{EFF}}$  and temperature (Figures 5 and 6).

The observation that  $\text{NO}_3^-$  increases with distance downstream of the WWTP in the absence of effluent but not upstream of the WWTP strongly suggests that this material is associated with effluent discharge, perhaps material stored in the sediments from years of high N loading from nutrient rich effluent. Future studies which examine the spatial extent to which the WWTP's loads have affected sediment N pools and thus benthic N fluxes would help evaluate the speed and extent to which ecological processes in downstream aquatic ecosystems might respond to management of point sources of nitrogen.

#### 4.3. Environmental Controls on Nitrate Concentration

Given that our data suggest multiple processes control the concentration of  $\text{NO}_3^-$  in this reach of the Sacramento River, we sought to better understand how these processes interact and how they respond to environmental controls such as flow and thus travel time, temperature and turbidity. Laboratory and bottle incubation studies have suggested these environmental controls affect nitrification (Damashek et al., 2016, and reference therein). Other studies and streams have shown that these environmental controls affect nutrient spiraling and the fate of anthropogenic nitrogen inputs (e.g., Ensign & Doyle, 2006; Hensley et al., 2015; Pennino et al., 2016; Wollheim et al., 2008).

##### 4.3.1. Travel Time

We hypothesized that travel time—a direct function of river discharge—may be an important control on both nitrification and benthic processes because it determines the amount of time the microbial community has to respond to the abrupt increase in  $\text{NH}_4^+$  concentration that occurs just below FPT and because it alters the time available for interaction with the benthos. In the United States, effluent is chlorinated/dechlorinated prior to being discharged to the river, thus the effluent itself is unlikely to be a source of nitrifiers, as has been reported in several recent studies (Aissa-Grouz et al., 2016; Raimonet et al., 2015), and there may be a lag period during which pelagic nitrifier populations grow in response to the point source addition of  $\text{NH}_4^+$  (Andersson et al., 2006; Damashek et al., 2016). Alternatively, because this section of the river typically experiences high  $\text{NH}_4^+$  conditions, it seemed possible that there would be a sufficient source of nitrifiers in the sediment that could not only act at the sediment-water interface but may also inoculate the water column due to turbulence and suspension (Damashek et al., 2016).

To assess the role of travel time,  $T$ , we examined its relationship with  $R_{\Delta\text{NO}_3^-}^{+\text{EFF}}$  and  $R_{\text{Nitrific}}$ . We found no significant relationship between  $T$  and either of these rates (supporting information Figure S5), suggesting that time is not necessary to activate the nitrifier community; this community may be present at relatively high abundance in the river, particularly in sediments below the WWTP that typically experience high  $\text{NH}_4^+$  concentrations. These nitrifiers can be easily entrained into the water column from the sediment even under moderate discharge rates.

##### 4.3.2. Turbidity

A number of studies have shown a strong relationship between nitrification and water column suspended sediment concentrations (Damashek et al., 2016; Hsiao et al., 2014; Xia et al., 2013). Higher suspended sediment concentrations are associated with resuspension of nitrifiers into the water column, and studies have shown that the sediment itself also provides additional substrate that can support bacterial growth (Hsiao

et al., 2014; Iriarte et al., 1998). With the exception of higher turbidity associated with the high flow storm events that were removed from our analysis due to low travel times between the stations, in this study turbidity was relatively constant ( $\sim 2\text{--}15$  FNU) throughout the study period, corresponding to a suspended sediment concentration of  $10\text{--}30$  mg L $^{-1}$  (supporting information Figure S4), thus no clear conclusions can be drawn from this study about the effects of turbidity on nitrification rates.

#### 4.3.3. Temperature

The most significant environmental control we found in our study was temperature (Figures 5 and 6). Higher temperatures favor faster reaction kinetics and faster growth rates of microbial populations, including nitrifiers, and numerous studies have documented the effect of temperature on nitrification rates (e.g., Damashek et al., 2016, and references therein; Strauss et al., 2004). Optimal temperatures for activity and growth of nitrifiers are believed to be between 20 and 35°C (Raimonet et al., 2015). We found lowest  $R_{\Delta\text{NO}_3}$  values ( $\sim 1.5$   $\mu\text{M d}^{-1}$ ) occurred when temperatures were less than 15°C, while higher  $R_{\text{nitrific}}$  values (2.5–3.5  $\mu\text{M d}^{-1}$ ) occurred when temperatures exceeded 15°C.

Similarly,  $R_{\Delta\text{NO}_3}^{+EFF}$  values were notably higher in the warmer summer months ( $\sim 5\text{--}8$   $\mu\text{M d}^{-1}$ ), with the coldest winter months (November and December) showing little change or even small  $\text{NO}_3^-$  losses (Figure 3c). Interestingly, the slope of the relationship between temperature and  $R_{\Delta\text{NO}_3}$  observed under both +EFF and -EFF conditions was notably steeper than for  $R_{\text{Nitrif.E}}$  (Figures 5 and 6). This indicates that warmer temperatures have less of an effect on one or more processes that remove  $\text{NO}_3^-$  (like uptake and denitrification) compared to processes that contribute to the  $\text{NO}_3^-$  pool (like whole system nitrification and release of  $\text{NO}_3^-$  from the benthos), resulting in the net effect of temperature being greater on these combined processes than on nitrification of effluent-derived  $\text{NH}_4^+$ . This unexpected finding warrants further investigation, especially considering the effects of temperature on  $\text{NH}_4^+$  and  $\text{NO}_2^-$  oxidation have been found to differ (Schaefer & Hollibaugh, 2017). In this section of the Sacramento River,  $\text{NO}_2^-$  concentrations were found to increase with downstream travel, suggesting  $\text{NH}_4^+$  oxidation rates are greater than  $\text{NO}_2^-$  oxidation rates (Kraus et al., 2017b).

## 5. Conclusions and Ecological Implications

Our results regarding nitrification rates have important ecological implications. After only  $\sim 2$  days of downstream travel, nitrification of effluent-derived  $\text{NH}_4^+$  accounted for up to 50% of the  $\text{NO}_3^-$  in the river (Table 1 and supporting information S7). As nitrification proceeds in the downstream estuary, the fraction of the total  $\text{NO}_3^-$  pool that can be attributed to recent effluent inputs versus other sources would increase. This highlights the importance of effluent contributions of  $\text{NH}_4^+$  and rates of nitrification in determining the size of both the  $\text{NH}_4^+$  and  $\text{NO}_3^-$  pools in the estuary (Dahm et al., 2016; Novick et al., 2015). In particular, during nonstorm periods, when upstream  $\text{NO}_3^-$  concentrations are low and residence times are longer, much of the  $\text{NO}_3^-$  entering the Delta, as well as the downstream regions of the estuary, originates from nitrogen originally discharged from the WWTP as  $\text{NH}_4^+$ . This has important repercussions for future nutrient supplies to the estuary, especially in light of forthcoming upgrades to Sacramento's WWTP that are expected to dramatically decrease total N inputs by 2021 (Dahm et al., 2016; Kraus et al., 2017a, 2017b; Novick et al., 2015).

Using rates estimated in this study, we can approximate the amount of time it would take  $\text{NH}_4^+$  present in the river to be converted to  $\text{NO}_3^-$  via nitrification. Assuming river  $\text{NH}_4^+$  concentrations ranging from 20 to 100  $\mu\text{M}$ , a nitrification rate of  $0.5$   $\mu\text{M d}^{-1}$  would take from 40 to 200 days, while a nitrification rate of  $3.5$   $\mu\text{M d}^{-1}$  would take from 6 to 28 days to deplete the  $\text{NH}_4^+$  pool (supporting information Figure S6). Transit times through the Delta are more on the order of weeks (Downing et al., 2016; Jassby, 2008; Schoellhamer et al., 2016). This highlights that the nitrification rates found in our study could appreciably attenuate concentrations of effluent-derived  $\text{NH}_4^+$ , with the extent dependent on residence times within the system and reaction kinetics. Thus, depending on the region of interest and flow conditions, this could result in either high or negligible concentrations of  $\text{NH}_4^+$ , which underscores the benefits of understanding both concentrations and rates of change of nutrient pools. Moreover, this estimate is mainly heuristic, as it has been shown by Damashek et al. (2014, 2016) that nitrification rates in the estuary vary spatially, and were significantly affected by temperature, suspended particulate matter concentrations, as well as  $\text{NH}_4^+$  concentration and differences in microbial community abundance and composition.

Results from this study also revealed the importance of benthic N pools and dynamics. We have shown that elevated  $\text{NO}_3^-$  efflux is associated with effluent inputs under warmer conditions, although—as we point out

above—the spatial extent of this effect is unknown. Relatively few studies have characterized benthic flux rates for  $\text{NO}_3^-$  and  $\text{NH}_4^+$  in this system (Cornwell et al., 2014; Kuwabara et al., 2009), and to our knowledge no studies in this system nor any other system have explicitly attempted to associate the magnitudes of these fluxes to the proximity of wastewater effluent release. This remains a critical gap in our knowledge.

Our results highlight the need to keep in mind all of the factors that affect nitrification rates, as well as other sources and sinks for  $\text{NH}_4^+$  and  $\text{NO}_3^-$ . For example, as Sacramento River water enters the Delta there are changes in chemical and physical properties (e.g., temperature, salinity, turbidity, dissolved oxygen, and turbulence) which can affect processes like nitrification (Andersson et al., 2006; Bernhard & Bollmann, 2010; de Bie et al., 2002). Mixing of different source waters could also affect nutrient concentrations and the composition and abundance of the nitrifying community, and at lower concentrations of  $\text{NH}_4^+$  nitrification rates may be lower due to substrate limitation (Damaskos et al., 2014, 2016; de Bie et al., 2002). Phytoplankton uptake of  $\text{NH}_4^+$  will likely shorten the time it takes for  $\text{NH}_4^+$  to be drawn down, however, Parker et al. (2012) estimated that uptake by phytoplankton likely accounts for less than 15% of  $\text{NH}_4^+$  losses in the Delta, and thus is a less significant biological process affecting the fate of  $\text{NH}_4^+$  than nitrification. Interaction with wetland habitats adds another layer of complexity: although most wetlands are a net sink for nutrients, they can also be a source (Fisher & Acreman, 2004). A study by Strauss et al. (2004) suggests that benthic nitrification rates in sediment were higher in backwater, shallow water regions compared to the channelized section of the Mississippi River. Similarly, Downing et al. (2016) found that net ecosystem  $\text{NO}_3^-$  loss rates varied spatially in the northern Delta, likely as a function of aquatic habitat. Finally, many of the environmental factors affecting N cycling in this system will be altered by changes in both human and natural forcings, including changes to flow that could alter water residence times, higher temperatures that may increase biogeochemical transformation rates, and restoration of wetlands that may increase sinks for nitrogen (Dahm et al., 2016).

This study demonstrates how a network of real time, continuous water quality stations, with sensors reporting high frequency nutrient concentration data, captures both nutrient concentrations and rates of nutrient processing, providing information over broad temporal and spatial scales in ways not previously feasible (Bergamaschi et al., 2017; Blaen et al., 2016; Heffernan & Cohen, 2010; Pellerin et al., 2016; Rode et al., 2016b). Conducting similar studies in other systems as well as in other areas of the Delta and greater San Francisco Estuary will help illuminate the effects of effluent additions on aquatic systems, as it relates to both water column and benthic processes. Conducting studies with simultaneous continuous measurements of  $\text{NO}_3^-$ ,  $\text{NH}_4^+$ , and  $\text{PO}_4^{3-}$  along with other water quality measurements will further that knowledge. This approach can be broadly applied to other systems, capturing a range of environmental settings and quantifying rates across different types of aquatic habitats. Such information will improve our ability to understand and manage both natural and anthropogenic impacts on aquatic ecosystems.

#### Acknowledgments

Funding for this study was provided by Sacramento Regional County Sanitation District (SRCSD; grant 13WSCA600000947/90000080), U.S. Bureau of Reclamations (BOR; grant 13WSCA4600010038/4600010038), and the U.S. Geological Survey Cooperative Water Program. This project was only possible due to the USGS California Water Science Center's Biogeochemistry and Hydrodynamic Group staff who maintain the continuous water quality monitoring stations, and to Erwin Van Nieuwenhuysen at BOR and both Lisa Thompson and Timothy Mussen at Sacramento Regional County Sanitation District for supporting these stations. We also thank Dave Evans for help with data analysis. All data used in this study are available at <http://waterdata.usgs.gov/usa/nwis>. Please see supporting information for additional figures and tables.

#### References

- Aissa-Grouz, N., Garnier, J., Billen, G., Mercier, B., & Martinez, A. (2016). The response of river nitrification to changes in wastewater treatment (The case of the lower Seine River downstream from Paris). *Annales de Limnologie - International Journal of Limnology*, 51(4), 351–364. <https://doi.org/10.1051/limn/2015031>
- Alexander, R. B., Böhlke, J. K., Boyer, E. W., David, M. B., Harvey, J. W., Mulholland, P. J., ... Wollheim, W. M. (2009). Dynamic modeling of nitrogen losses in river networks unravels the coupled effects of hydrological and biogeochemical processes. *Biogeochemistry*, 93(1–2), 91–116. <https://doi.org/10.1007/s10533-008-9274-8>
- Andersson, M. G. I., Brion, N., & Middelburg, J. J. (2006). Comparison of nitrifier activity versus growth in the Scheldt estuary—A turbid, tidal estuary in northern Europe. *Aquatic Microbial Ecology*, 42(2), 149–158. <https://doi.org/10.3354/ame042149>
- Bende-Michl, U., Verburg, K., & Cresswell, H. P. (2013). High-frequency nutrient monitoring to infer seasonal patterns in catchment source availability, mobilisation and delivery. *Environmental Monitoring and Assessment*, 185(11), 9191–9219. <https://doi.org/10.1007/s10661-013-3246-8>
- Bergamaschi, B. A., Downing, B. D., Kraus, T. E. C., & Pellerin, B. A. (2017). *Designing a high-frequency nutrient and biogeochemical monitoring network for the Sacramento/San Joaquin Delta, northern California* (Scientific Investigation Rep. 2017-5058, 40 p.). Reston, VA: U.S. Geological Survey. <https://doi.org/10.3133/sir20175058>
- Bernhard, A. E., & Bollmann, A. (2010). Estuarine nitrifiers: New players, patterns and processes. *Estuarine, Coastal and Shelf Science*, 88(1), 1–11. <https://doi.org/10.1016/j.ecss.2010.01.023>
- Bernhardt, E. S., & Likens, G. E. (2002). Dissolved organic carbon enrichment alters nitrogen dynamics in a forest stream. *Ecology*, 83(6), 1689–1700. [https://doi.org/10.1890/0012-9658\(2002\)083\[1689:DOCEAN\]2.0.CO;2](https://doi.org/10.1890/0012-9658(2002)083[1689:DOCEAN]2.0.CO;2)
- Bianchi, M., Feliatra, D., & Lefevre, (1999). Regulation of nitrification in the land-ocean contact area of the Rhone River plume (NW Mediterranean). *Aquatic Microbial Ecology*, 18(3), 301–312.
- Blaen, P. J., Khamis, K., Lloyd, C. E., Bradley, C., Hannah, D., & Krause, S. (2016). Real-time monitoring of nutrients and dissolved organic matter in rivers: Capturing event dynamics, technological opportunities and future directions. *Science of the Total Environment*, 569–570, 647–660. <https://doi.org/10.1016/j.scitotenv.2016.06.116>

- Carey, R. O., & Migliaccio, K. W. (2009). Contribution of wastewater treatment plant effluents to nutrient dynamics in aquatic systems: A review. *Environmental Management*, 44(2), 205–217. <https://doi.org/10.1007/s00267-009-9309-5>
- Carini, S. A., McCarthy, M. J., & Gardner, W. S. (2010). An isotope dilution method to measure nitrification rates in the northern Gulf of Mexico and other eutrophic waters. *Continental Shelf Research*, 30(17), 1795–1801. <https://doi.org/10.1016/j.csr.2010.08.001>
- Constable, M., Charlton, M., Jensen, F., McDonald, K., Craig, G., & Taylor, K. W. (2003). An ecological risk assessment of ammonia in the aquatic environment. *Human and Ecological Risk Assessment: An International Journal*, 9(2), 527–548. <https://doi.org/10.1080/713609921>
- Cornwell, J. C., Glibert, P. M., & Owens, M. S. (2014). Nutrient fluxes from sediments in the San Francisco Bay Delta. *Estuaries and Coasts*, 37(5), 1120–1133. <https://doi.org/10.1007/s12237-013-9755-4>
- Crawford, J. T., Loken, L. C., Casson, N. J., Smith, C., Stone, A. G., & Winslow, L. A. (2015). High-speed limnology: Using advanced sensors to investigate spatial variability in biogeochemistry and hydrology. *Environmental Science and Technology*, 49(1), 442–450. <https://doi.org/10.1021/es504773x>
- Dahm, C. N., Parker, A. E., Adelson, A. E., Christman, M. A., & Bergamaschi, B. A. (2016). Nutrient dynamics of the Delta: Effects on primary producers. *San Francisco Estuary and Watershed Science*, 14(4), 1–35. <https://doi.org/10.15447/sfews.2016v14iss4art4>
- Dai, M., Wang, L., Guo, X., Zhai, W., Li, Q., He, B., & Kao, S. J. (2008). Nitrification and inorganic nitrogen distribution in a large perturbed river/estuarine system: The Pearl River Estuary, China. *Biogeosciences*, 5(5), 1227–1244. <https://doi.org/10.5194/bg-5-1227-2008>
- Damashek, J., Casciotti, K. L., & Francis, C. A. (2016). Variable nitrification rates across environmental gradients in turbid, nutrient-rich estuarine waters of San Francisco Bay. *Estuaries and Coasts*, 39(4), 1050–1071. <https://doi.org/10.1007/s12237-016-0071-7>
- Damashek, J., Smith, J. M., Mosier, A. C., & Francis, C. A. (2014). Benthic ammonia oxidizers differ in community structure and biogeochemical potential across a riverine delta. *Frontiers in Microbiology*, 5, 743. <https://doi.org/10.3389/fmicb.2014.00743>
- de Bie, M. J. M., Starink, M., Boschker, H. T. S., Peene, J. J., & Laanbroek, H. J. (2002). Nitrification in the Schelde estuary: Methodological aspects and factors influencing its activity. *FEMS Microbiology Ecology*, 42(1), 99–107. [https://doi.org/10.1016/s0168-6496\(02\)00325-2](https://doi.org/10.1016/s0168-6496(02)00325-2)
- Downing, B. D., Bergamaschi, B. A., Kendall, C., Kraus, T. E., Dennis, K. J., Carter, J. A., & Von Dessonneck, T. S. (2016). Using continuous underway isotope measurements to map water residence time in hydrodynamically complex tidal environments. *Environmental Science and Technology*, 50(24), 13387–13396. <https://doi.org/10.1021/acs.est.6b05745>
- Downing, B. D., Bergamaschi, B. A., & Kraus, T. E. C. (2017). Synthesis of data from high frequency nutrient and associated biogeochemical monitoring for the Sacramento-San Joaquin Delta, northern California (U.S. Geological Survey Scientific Investigations Rep. 2017-5066, 28 pp.). Reston, VA: U.S. Geological Survey. <https://doi.org/10.3133/sir20175066>
- Dugdale, R. C., Wilkerson, F. P., Hogue, V. E., & Marchi, A. (2007). The role of ammonium and nitrate in spring bloom development in San Francisco Bay. *Estuarine, Coastal and Shelf Science*, 73(1–2), 17–29. <https://doi.org/10.1016/j.ecss.2006.12.008>
- Ensign, S. H., & Doyle, M. W. (2006). Nutrient spiraling in streams and river networks. *Journal of Geophysical Research*, 111, G04009. <https://doi.org/10.1029/2005JG000114>
- Faunt, C. C. (Ed.). (2009). Groundwater availability of the Central Valley Aquifer, California (U.S. Geological Survey Professional Pap. 1766, 225 pp.). Reston, VA: U.S. Geological Survey. Retrieved from <https://pubs.usgs.gov/pp/1766/?version=meter+at+null&module=meter-Links&pgtype=Blogs&contentId=&mediaId=&referrer=&priority=true&action=click&contentCollection=meter-links-click>
- Fisher, J., & Acreman, M. (2004). Wetland nutrient removal: a review of the evidence. *Hydrology and Earth System Sciences Discussions*, 8(4), 673–685.
- Foe, C., Ballard, A., & Fong, S. (2010). Nutrient concentrations and biological effects in the Sacramento-San Joaquin Delta (report, 90 pp.). Rancho Cordova, CA: Central Valley Regional Control Board. Retrieved from [http://www.waterboards.ca.gov/rwqcb5/water\\_issues/delta\\_water\\_quality/ambient\\_ammonia\\_concentrations/foe\\_nutrient\\_conc\\_bio\\_effects.pdf](http://www.waterboards.ca.gov/rwqcb5/water_issues/delta_water_quality/ambient_ammonia_concentrations/foe_nutrient_conc_bio_effects.pdf)
- Garnier, J., Billen, G., & Cebron, A. (2007). Modelling nitrogen transformations in the lower Seine river and estuary (France): Impact of wastewater release on oxygenation and N<sub>2</sub>O emission. *Hydrobiologia*, 588(1), 291–302. <https://doi.org/10.1007/s10750-007-0670-1>
- Gilbert, M., Needoba, J., Koch, C., Barnard, A., & Baptista, A. (2013). Nutrient loading and transformations in the Columbia River Estuary determined by high-resolution in situ sensors. *Estuaries and Coasts*, 36(4), 708–727. <https://doi.org/10.1007/s12237-013-9597-0>
- Glibert, P. M., Wilkerson, F. P., Dugdale, R. C., Raven, J. A., Dupont, C. L., Leavitt, P. R., ... Kana, T. M. (2016). Pluses and minuses of ammonium and nitrate uptake and assimilation by phytoplankton and implications for productivity and community composition, with emphasis on nitrogen-enriched conditions. *Limnology and Oceanography*, 61(1), 165–197. <https://doi.org/10.1002/lo.10203>
- Godin, G. (1972). *The analysis of tides* (264 pp.). University of Toronto Press.
- Heffernan, J. B., & Cohen, M. J. (2010). Direct and indirect coupling of primary production and diel nitrate dynamics in a subtropical spring-fed river. *Limnology and Oceanography*, 55(2), 677–688. <https://doi.org/10.4319/lo.2010.55.2.00677>
- Hensley, R. T., Cohen, M. J., & Korhnak, L. V. (2014). Inferring nitrogen removal in large rivers from high-resolution longitudinal profiling. *Limnology and Oceanography*, 59(4), 1152–1170. <https://doi.org/10.4319/lo.2014.59.4.1152>
- Hensley, R. T., Cohen, M. J., & Korhnak, L. V. (2015). Hydraulic effects on nitrogen removal in a tidal spring-fed river. *Water Resources Research*, 51, 1443–1456. <https://doi.org/10.1002/2014WR016178>
- Hsiao, S. S. Y., Hsu, T.-C., Liu, J.-W., Xie, X., Zhang, Y., Lin, J., ... Kao, S.-J. (2014). Nitrification and its oxygen consumption along the turbid Chang Jiang River plume. *Biogeosciences*, 11(7), 2083–2098. <https://doi.org/10.5194/bg-11-2083-2014>
- Iriarte, A., de la Sota, A., & Orive, E. (1998). Seasonal variation of nitrification along a salinity gradient in an urban estuary. *Hydrobiologia*, 362(1–3), 115–126.
- Jassby, A. D. (2008). Phytoplankton in the Upper San Francisco Estuary: Recent biomass trends, their causes and their trophic significance. *San Francisco Estuary and Watershed Science*, 6(1), Article 2.
- Kendall, C., Young, M. B., Silva, S. R., Kraus, T. E. C., Peek, S., & Guerin, M. (2015). Tracing nutrient and organic matter sources and biogeochemical processes in the Sacramento River and Northern Delta: proof of concept using stable isotope data. Reston, VA: U.S. Geological Survey. Retrieved from <http://water.usgs.gov/hrp/isotope-tracers/san-francisco-bay-estuary.html>
- Kirchner, J. W., Feng, X., Neal, C., & Robson, A. J. (2004). The fine structure of water-quality dynamics: The (high-frequency) wave of the future. *Hydrological Processes*, 18(7), 1353–1359. <https://doi.org/10.1002/hyp.5537>
- Kratzer, C. R., Kent, R., Seleh, D. K., Knifong, D. L., Dileanis, P. D., & Orlando, J. L. (2011). Trends in nutrient concentrations, loads, and yields in streams in the Sacramento, San Joaquin, and Santa Ana Basins, California, 1975–2004 (Rep. 2010-5228, 112 pp.). Reston, VA: U.S. Geological Survey. Retrieved from <https://pubs.usgs.gov/sir/2010/5228/>
- Kraus, T. E. C., Bergamaschi, B. A., & Downing, B. D. (2017a). An introduction to high-frequency nutrient and biogeochemical monitoring for the Sacramento–San Joaquin Delta, northern California (U.S. Geological Survey Scientific Investigations Rep. 2017–2071, 42 pp.). Reston, VA: U.S. Geological Survey. <https://doi.org/10.3133/sir20175071>

- Kraus, T. E. C., Carpenter, K. D., Bergamaschi, B. A., Parker, A. E., Stumpner, E., Downing, B. D., . . . Mussen, T. D. (2017b). A river-scale Lagrangian experiment examining controls on phytoplankton dynamics in the presence and absence of treated wastewater effluent high in ammonium. *Limnology and Oceanography*, 62(3), 1234–1253. <https://doi.org/10.1002/limo.10497>
- Kunz, J. V., Hensley, R., Bräse, L., Borchardt, D., & Rode, M. (2017). High frequency measurements of reach scale nitrogen uptake in a fourth order river with contrasting hydromorphology and variable water chemistry (Weiße Elster, Germany). *Water Resources Research*, 53, 328–343. <https://doi.org/10.1002/2016WR019355>
- Kuwabara, J. S., Topping, B. R., Parchaso, F., Engelstad, A. C., & Greene, V. E. (2009). Benthic flux of nutrients and trace metals in the northern component of San Francisco Bay, California (U.S. Geological Survey Open-File Rep. 2009-1286, 14 pp.). Reston, VA: U.S. Geological Survey.
- Lehman, P. W., Kendall, C., Guerin, M. A., Young, M. B., Silva, S. R., Boyer, G. L., & Teh, S. J. (2015). Characterization of the microcystis bloom and its nitrogen supply in San Francisco Estuary using stable isotopes. *Estuaries and Coasts*, 38(1), 165–178. <https://doi.org/10.1007/s12237-014-9811-8>
- Luoma, S. N., Dahm, C. N., Healey, M., & Moore, J. N. (2015). Water and the Sacramento-San Joaquin Delta: Complex, chaotic, or simply can-tankerous? *San Francisco Estuary and Watershed Science*, 13(3), Article 7. <https://doi.org/0.15447/sfews.2015v13iss3art7>
- Mulholland, P. J., Hall, R. O., Sobota, D. J., Dodds, W. K., Findlay, S. E., Grimm, N. B., . . . Tank, J. L. (2009). Nitrate removal in stream ecosystems measured by 15N addition experiments: Denitrification. *Limnology and Oceanography*, 54(3), 666–680.
- Novick, E., Holleman, R., Jabusch, T., Sun, J., Trowbridge, P., Senn, D., . . . Peek, S. (2015). *Characterizing and quantifying nutrient sources, sinks and transformations in the Delta: Synthesis, modeling, and recommendations for monitoring* (p. 28). San Francisco Estuary Institute. Retrieved from <http://www.sfei.org/documents/characterizing-and-quantifying-nutrient-sources-sinks-and-transformations-delta-synthesis>
- O'Donnell, K. (2014). *Nitrogen sources and transformations along the Sacramento River: Linking wastewater effluent releases to downstream nitrate* (52 pp.). Sacramento, CA: California State University.
- Owens, N. J. (1986). Estuarine nitrification: A naturally occurring fluidized bed reaction? *Estuarine, Coastal and Shelf Science*, 22(1), 31–44.
- Paerl, H. W., Hall, N. S., Peierls, B. L., & Rossignol, K. L. (2014). Evolving paradigms and challenges in estuarine and coastal eutrophication dynamics in a culturally and climatically stressed world. *Estuaries and Coasts*, 37(2), 243–258. <https://doi.org/10.1007/s12237-014-9773-x>
- Paerl, H. W., & Scott, J. T. (2010). Throwing fuel on the fire: Synergistic effects of excessive nitrogen inputs and global warming on harmful algal blooms. *Environmental Science and Technology*, 44(20), 7756–7758. <https://doi.org/10.1021/es102665e>
- Paerl, H. W., Scott, J. T., McCarthy, M. J., Newell, S., Gardner, E. W., Havens, K. E., . . . Wurtsbaugh, W. A. (2016). It takes two to tango: When and where dual nutrient (N & P) reductions are needed to protect lakes and downstream ecosystems. *Environmental Science and Technology*, 50(20), 10805–10813.
- Parker, A. E., Dugdale, R. C., & Wilkerson, F. P. (2012). Elevated ammonium concentrations from wastewater discharge depress primary productivity in the Sacramento River and the Northern San Francisco Estuary. *Marine Pollution Bulletin*, 64(3), 574–586. <https://doi.org/10.1016/j.marpolbul.2011.12.016>
- Pellerin, B. A., Bergamaschi, B. A., Downing, B. D., Saraceno, J. F., Garrett, J. A., & Olsen, L. D. (2013). Optical techniques for the determination of nitrate in environmental waters: Guidelines for instrument selection, operation, deployment, maintenance, quality assurance, and data reporting (U.S. Geological Survey Techniques and Methods, 1-D5, 37 pp.). Reston, VA: U.S. Geological Survey.
- Pellerin, B. A., Bergamaschi, B. A., Gilliom, R. J., Crawford, C. G., Saraceno, J., Frederick, C. P., . . . Murphy, J. C. (2014). Mississippi River nitrate loads from high frequency sensor measurements and regression-based load estimation. *Environmental Science and Technology*, 48(21), 12612–12619. <https://doi.org/10.1021/es504029c>
- Pellerin, B. A., Downing, B. D., Kendall, C., Dahlgren, R. A., Kraus, T. E. C., Saraceno, J., . . . Bergamaschi, B. A. (2009). Assessing the sources and magnitude of diurnal nitrate variability in the San Joaquin River (California) with an in situ optical nitrate sensor and dual nitrate isotopes. *Freshwater Biology*, 54(2), 376–387.
- Pellerin, B. A., Stauffer, B. A., Young, D. A., Sullivan, D. J., Bricker, S. B., Walbridge, M. R., . . . Shaw, D. M. (2016). Emerging tools for continuous nutrient monitoring networks: Sensors advancing science and water resources protection. *Journal of the American Water Resources Association*, 52(4), 993–1008. <https://doi.org/10.1111/1752-1688.12386>
- Pennino, M. J., Kaushal, S. S., Murthy, S. N., Blomquist, J. D., Cornwell, J. C., & Harris, L. A. (2016). Sources and transformations of anthropogenic nitrogen along an urban river-estuarine continuum. *Biogeosciences*, 13(22), 6211–6228. <https://doi.org/10.5194/bg-13-6211-2016>
- Peterson, B. J., Wollheim, W. M., Mulholland, P. J., Webster, J. R., Meyer, J. L., Tank, J. L., . . . Hershey, A. E. (2001). Control of nitrogen export from watersheds by headwater streams. *Science*, 292(5514), 86–90.
- Raimonet, M., Vilmin, L., Flipo, N., Rocher, V., & Laverman, A. M. (2015). Modelling the fate of nitrite in an urbanized river using experimentally obtained nitrifier growth parameters. *Water Research*, 73, 373–387. <https://doi.org/10.1016/j.watres.2015.01.026>
- Randall, D., & Tsui, T. (2002). Ammonia toxicity in fish. *Marine Pollution Bulletin*, 45(1), 17–23.
- Rode, M., Halbedel Nee Angelstein, S., Anis, M. R., Borchardt, D., & Weitere, M. (2016a). Continuous in-stream assimilatory nitrate uptake from high-frequency sensor measurements. *Environmental Science and Technology*, 50(11), 5685–5694. <https://doi.org/10.1021/acs.est.6b00943>
- Rode, M., Wade, A. J., Cohen, M. J., Hensley, R. T., Bowes, M. J., Kirchner, J. W., . . . Jomaa, S. (2016b). Sensors in the stream: The high-frequency wave of the present. *Environmental Science and Technology*, 50(19), 10297–10307. <https://doi.org/10.1021/acs.est.6b02155>
- Rusjan, S., & Mikos, M. (2010). Seasonal variability of diurnal in-stream nitrate concentration oscillations under hydrologically stable conditions. *Biogeochemistry*, 97(2–3), 123–140. <https://doi.org/10.1007/s10533-009-9361-5>
- Saleh, D., & Domagalski, J. (2015). SPARROW modeling of nitrogen sources and transport in rivers and streams of California and adjacent states, U.S. *Journal of the American Water Resources Association*, 51(6), 1487–1507. <https://doi.org/10.1111/1752-1688.12325>
- Schaefer, S. C., & Hollibaugh, J. T. (2017). Temperature decouples ammonium and nitrite oxidation in coastal waters. *Environmental Science and Technology*, 51(6), 3157–3164.
- Schoellhamer, D. H., Wright, S. A., Monismith, S. G., & Bergamaschi, B. A. (2016). Advances in understanding flow dynamics and transport of water-quality constituents in the Sacramento-San Joaquin River Delta. *San Francisco Estuary and Watershed Science*, 14(4), Article 1. <https://doi.org/10.15447/sfews.2016v14iss4art1>
- Schlegel, B., & Domagalski, J. L. (2016). Riverine nutrient trends in the Sacramento and San Joaquin Basins, California: A comparison to state and regional water quality policies. *San Francisco Estuary and Watershed Science*, 13(4). <http://dx.doi.org/10.15447/sfews.2015v13iss4art2>
- Shammas, N. K. (1986). Interactions of temperature, pH, and biomass on the nitrification process. *Journal of Water Pollution Control Federation*, 58(1), 52–59.
- Statham, P. J. (2012). Nutrients in estuaries—An overview and the potential impacts of climate change. *Science of the Total Environment*, 434, 213–227. <https://doi.org/10.1016/j.scitotenv.2011.09.088>

- Strauss, E. A., Mitchell, N. L., & Lamberti, G. A. (2002). Factors regulating nitrification in aquatic sediments: Effects of organic carbon, nitrogen availability, and pH. *Canadian Journal of Fisheries and Aquatic Sciences*, 59(3), 554–563.
- Strauss, E. A., Richardson, W. B., Bartsch, L. A., Cavanaugh, J. C., Bruesewitz, D. A., Imker, H., ... Soballe, D. M. (2004). Nitrification in the Upper Mississippi River: Patterns, controls, and contribution to the  $\text{NO}_3^-$ -budget. *Journal of the North American Benthological Society*, 23(1), 1–14. [https://doi.org/10.1899/0887-3593\(2004\)023<0001:NITUMR>2.0.CO;2](https://doi.org/10.1899/0887-3593(2004)023<0001:NITUMR>2.0.CO;2)
- Tank, J. L., Rosi-Marshall, E. J., Baker, M. A., & Hall, R. O. (2008). Are rivers just big streams? A pulse method to quantify nitrogen demand in a large river. *Ecology*, 89(10), 2935–2945.
- Wild-Allen, K., & Rayner, M. (2014). Continuous nutrient observations capture fine-scale estuarine variability simulated by a 3D biogeochemical model. *Marine Chemistry*, 167, 135–149. <https://doi.org/10.1016/j.marchem.2014.06.011>
- Wollheim, W. M., Vörösmarty, C. J., Bouwman, A. F., Green, P., Harrison, J., Linder, E., ... Syvitski, J. P. M. (2008). Global N removal by freshwater aquatic systems using a spatially distributed, within-basin approach. *Global Biogeochemical Cycles*, 22, GB2026. <https://doi.org/10.1029/2007GB002963>
- Xia, X., Li, S., & Shen, Z. (2008). Effect of nitrification on nitrogen flux across sediment-water interface. *Water Environment Research*, 80(11), 2175–2182. <https://doi.org/10.2175/106143008x296505>
- Xia, X., Liu, T., Yang, Z., Zhang, X., & Yu, Z. (2013). Dissolved organic nitrogen transformation in river water: Effects of suspended sediment and organic nitrogen concentration. *Journal of Hydrology*, 484, 96–104. <https://doi.org/10.1016/j.jhydrol.2013.01.012>
- Xia, X., Yang, Z., & Zhang, X. (2009). Effect of suspended-sediment concentration on nitrification in river water: Importance of suspended sediment-water interface. *Environmental Science and Technology*, 43(10), 3681–3687. <https://doi.org/10.1021/es8036675>